Biogeosystem Technique

Journal is being issued since 2014.
E-ISSN 2413-7316
2022. 9(2). Issued 2 times a year

Journal is indexed by: **Cross Ref** (USA), **Electronic scientific library** (Russia), **MIAR** (Spain), **Open Academic Journals Index** (USA), **CiteFactor – Directory of International Reseach Journals** (Canada).

All manuscripts are peer reviewed by experts in the respective field. Authors of the manuscripts bear responsibility for their content, credibility and reliability.

Editorial board doesn't expect the manuscripts' authors to always agree with its opinion.

Postal Address: 1717 N Street NW, Suite 1, Washington, District of Columbia 20036

Website: https://bgt.cherkasgu.press
E-mail: kalinitch@mail.ru

Founder and Editor: Cherkas Global University

Release date 25.12.2022
Format 21 × 29,7/4.

Headset Georgia.

Order № B-22.

Biogeosystem Technique

2022

Is. 2

C O N T E N T S

Articles

Published in the USA
Biogeosystem Technique
Issued since 2014.
E-ISSN: 2413-7316
2022. 9(2): 62-76

DOI: 10.13187/bgt.2022.2.62
https://bgt.cherkasgu.press

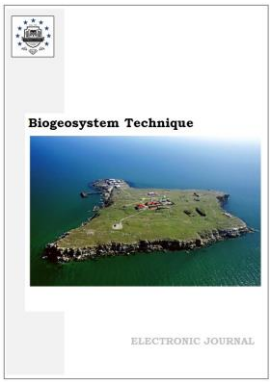

Articles

Interphase Nucleus and Transposable Elements (Review)

Tatiana T. Glazko [a], Galina V. Glazko [b], Gleb Yu. Kosovsky [a], Boris L. Zybaylov [b, *], Valery I. Glazko [a]

[a] FSBSI V.A. Afanasyev RI for Fur and Rabbit Farming, Moscow, Russian Federation
[b] University of Arkansas for Medical Sciences, Little Rock, AR, USA

Paper Review Summary:
Received: 2022, October 11
Received in revised form: 2022, November 18
Acceptance: 2022, December 16

Abstract

How the nuclear architectonic is influencing gene expression programs is a fast developing area of research. In this review we track the accumulated data about interphase nucleus architectonic and how it is changing in various cellular populations of eukaryotes. We also discuss in details how major structural components of chromosomes – centromeres and telomeres – are organized. They consist of tandem repeats and transposons, closely related with each other. Mobile genetic elements play a key role in creating ectopic chromosomal contacts and laminal attachments of genomic elements. We note that retrotransposons autonomous long repeats LINE and non-autonomous short repeats SINE are localized differently over chromosomes. LINEs are preferably located in heterochromatin while SINEs are associated with euchromatin. They are involved in nuclear architectonic dynamic while gene expression programs are changing. We also consider the data about retrotransposons' high evolutionary rate and their involvement into decreasing reproduction of inter-species hybrids. The relationship between genomic 'resistance' toward retrotransposition and the success insertion rate of several viruses is also discussed. The relationship between the variability of retrotranspositions, morphogenesis and speciation, as well as resistance to natural selection is a big question in contemporary medicine and biology given recent pandemic.

Keywords: Interphase nucleus, architectonic, hetero- and euchromatine, lamina, transposons, gene expression programs.

1. Introduction

Answering questions about the mechanisms of gene expression regulation, in particular epigenomics, is a top priority for contemporary biology. One of the most enigmatic questions is: what are the control mechanisms behind activation and termination of gene expression programs in different tissues and organs of multicellular organisms? While active studies of specific

* Corresponding author
E-mail addresses: blzybaylov@uams.edu (B.L. Zybaylov)

regulatory mechanisms, such as differential DNA and histone methylation, microRNA regulatory networks, are ongoing, the system regulation of gene expression programs remains poorly understood. The importance of understanding these mechanisms was obvious for a while already. Just to mention that aneuploidy – the balance change between chromosome dosages – leads to deep developmental damages, for example, trisomy of 13, 18 and 21 chromosomes result in Patau, Edwards and Down syndromes, respectively while, haploid chromosomal dosage preserves its ontogenetic potential (Li et al., 2014; Cui et al., 2020). Rapidly accumulating data suggests that system regulation of gene expression programs interaction and functioning is being affected via interphase nucleus architectonic.

2. Methods

Currently, the main and widely used methods of studying the architectonics of the interphase nuclei are Hi-C method and sites of chromatin interaction analysis by paired-end tag sequencing, that measure the 3D proximity of pairs of DNA loci by cross-linking, ligating, and sequencing the DNA. Using such methods, researchers have reconstructed the 3D conformation of chromatin in vivo in a wide variety of species in different cell types.

3. Discussion

Besides individual chromosomal territories interphase nucleus contains several other domains, some of them concentrating around nuclear periphery and some around the nucleolus, both in heterochromatin state, while others are located inside the nucleus and in euchromatine state (Figure 1).

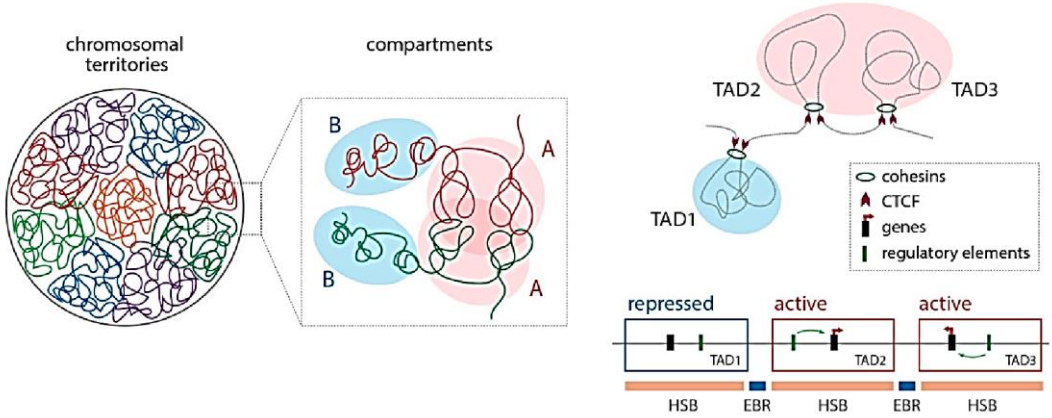

Fig. 1. Genomes are compartmentalized into different levels of organization, including: (i) chromosomal territories, (ii) 'open' (termed 'A')/'closed' (termed 'B') compartments inside chromosomal territories, (iii) topologically associated domains (TADs) and (iv) looping interactions.

TADs, which are delimited by insulating factors such as CTCF and cohesins, harbor looping topologies that permit long-range interactions between target genes and their distal enhancers, thus providing 'regulatory neighborhoods' within homologous syntenic blocks (HSBs). In this context, the integrative breakage model proposes that genomic regions involved in evolutionary reshuffling (evolutionary breakpoint regions, EBRs) that will be likely fixed within populations are (i) those that contain open chromatin DNA configurations and epigenetic features that could promote DNA accessibility and therefore genomic instability, and (ii) that do not interfere with essential genes and/or gene expression (Deakin et al., 2019).

Spatial positioning is a fundamental principle governing many processes in the nucleus. Chromatin is hierarchically organized, from nucleosomes to chromatin domains (CDs), or topologically associated domains (TADs), to higher-order compartments, the apex of which is chromosome territories (CT) (Figure 2).

Accumulating evidence suggests that chromatin organization is a critical factor in regulating gene expression. For example, enhancers interact with their target genes almost exclusively within the TAD, distally co-expressed genes are recruited into shared protein aggregates upon activation, and compact domains exhibit dynamic movement and configurational changes *in vivo*.

Nonrandom radial positioning of CTs in the nucleus suggest that there are preferential interaction patterns between chromosomal territories. These specific inter-chromosomal network patterns are changing during the cell cycle, cell differentiation as well as neoplastic transformation. The dynamics of these networks supposedly correlates with the global level of genome regulation. The proximity of certain chromosomal regions in cells (related to their genes co-expression), probably can explain the tendency for different translocations in pathologies.

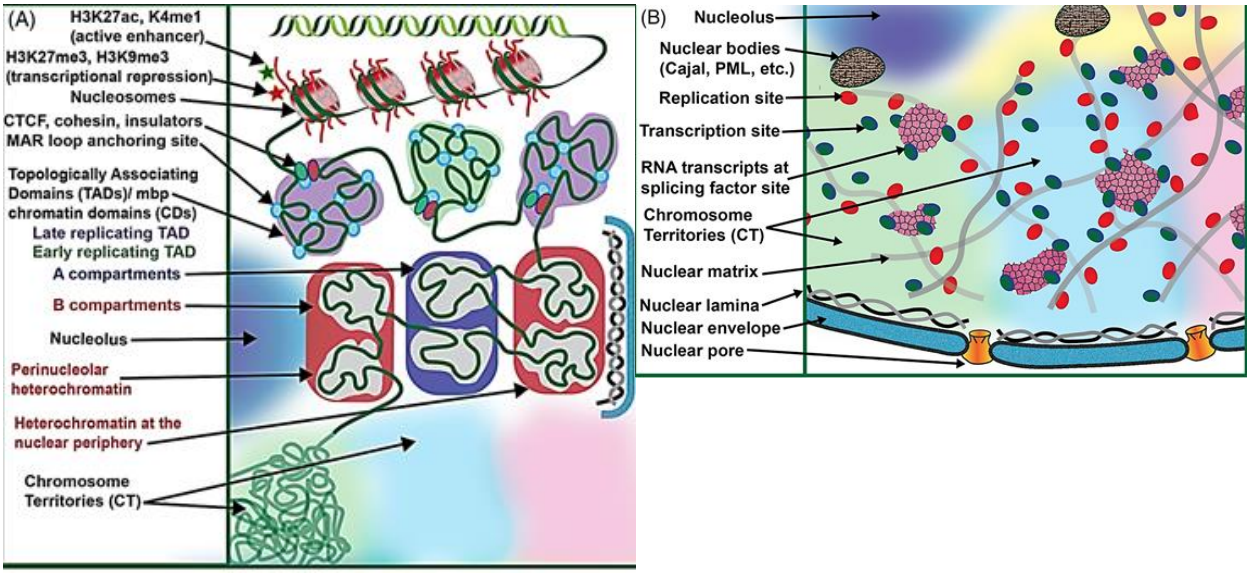

Fig. 2. Higher order chromatin organization and functioning nuclear architecture. A. Shows the hierarchical levels of chromatin organization, including: nucleosomes, chromatin fibers, chromatin loops, CD – chromatin domains, topologically associated domains (TADs), compartments A and B and chromosomal territories (CT). B. Functional nuclear architectonics.

Replication sites and nuclear accumulations of proteins are associated with the nuclear matrix. Transcription sites are associated with nuclear matrix or nuclear protein assemblies. Other nuclear bodies and structural elements of the nucleus are shown, such as the nuclear envelope, nuclear lamina, nuclear pore complex and nucleolus (Fritz et al., 2019).

Genomic regions, involved in evolutionary breakpoint regions (EBRs) are mostly divided into: (1) those, containing 'open' chromatin that allows easy DNA access for regulating genomic instabilities and (2) those, that do not interfere with gene expression and/or interactions (Deakin et al., 2019). Thus, it is imperative to understand underlying principles of the formation of these different genomic regions.

The most obvious eukaryotic chromosomal regions are telomeres and centromeres, playing the central role in interphase nucleus architectonic as well as meiosis and mitosis (Figure 3).

Telomeres consist of highly conserved microsatellite – a thousand-fold tandem repeat – hexanucleotide TTAGGG, which interacts with a number of proteins, protecting telomeres from damages and "illegitimate" fusion with other telomeres. These proteins are part of the shelterin protein complex, which facilitates the formation of a lasso-like structure to protect the open ends of telomeric DNA from damage (Shay, 2018). The protein complex consists of six shelterin members (Figures 4, 5) and includes TRF1 (telomeric repeat binding factor 1), which binds to the canonical TTAGGG double-stranded telomeric repeat and interacts with TIN2 (TRF1-interaction nuclear factor 2). Another shelterin protein is TRF2, which also binds double-stranded telomeric repeats and interacts with RAP1 (repressor/activator protein 1). POT1 (protection of telomeres 1) binds to TTAGGG single-stranded repeats and binds to TRF1 and TRF2 through a binding partner, TPP1, which also binds to TIN2.

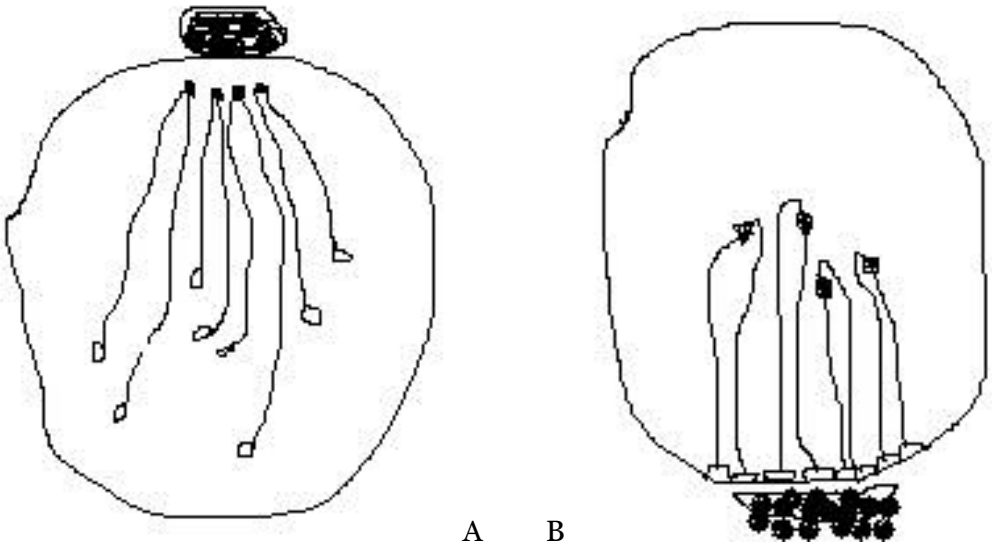

A B

Fig. 3. A – Telophase of mitosis with a restored nuclear envelope, centromeres (stained areas of chromosomes) accumulate towards the centrosome (accumulation of stained fragments on the nuclear envelope). B – Prophase I of meiosis, telomeres (unstained areas of chromosomes) accumulate on the nuclear envelope towards the centrosome (accumulation of colored fragments on the nuclear envelope).

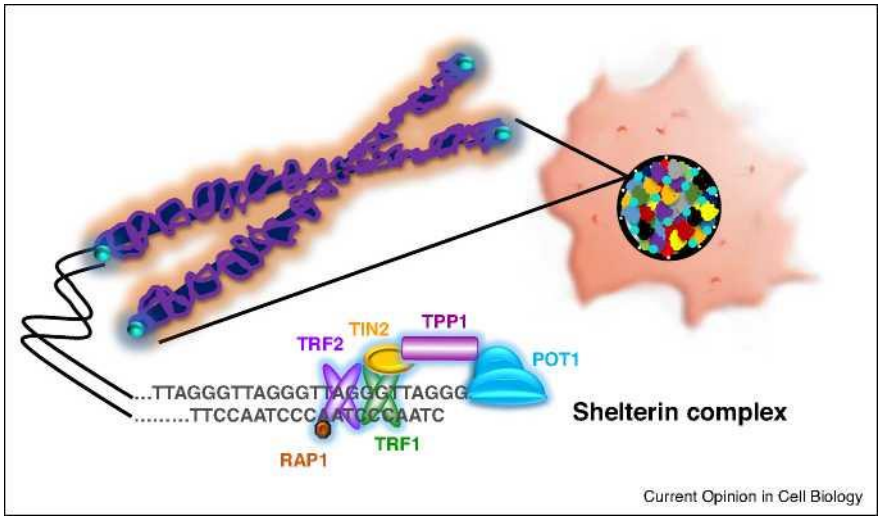

Fig. 4. Telomeres are repetitive DNA sequences at the ends of linear chromosomes

Telomeres are key elements of nuclear architectonics, determining the positioning of chromosomes in nuclear space and often associated with the nuclear envelope, and also protect the linear ends of chromosomes from DNA damage. The end of telomeric DNA consists of a single strand of G-rich DNA sequence forming a lasso-like structure, and this strand invades TTAGGG repeats to form a T-loop. In total, telomere ends make up only ~ 1/6000 of the total genomic DNA in a cell. Telomeres are gradually shortened with each cell division in the absence of a mechanism for maintaining telomeres, which ultimately leads to proliferation end. Loss of telomere protection can lead to a telomere damage, which can be overcome by the activation of telomerase (reverse transcriptase), which increases telomere repeats (Shay, 2018).

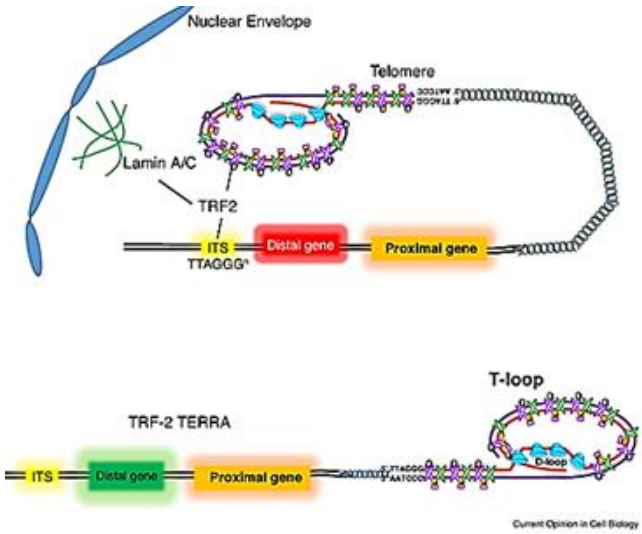

Fig. 5. Model of interactions between telomere and a distant gene

When cells have long telomeres, the 3D chromosomal loop positions the distal gene close to the telomere through interactions with interstitial telomere sequences (ITS), facilitated by shelterin proteins (such as TRF2) and proteins that are associated with the inner nuclear envelope (lamin A/C) ... The 3D telomere loop changes the chromatin structure near the distal gene, which leads to a change in gene expression. When cells have short telomeres, these associations are lost and distal gene expression is altered. There is also support for telomere repeat RNA (TERRA), which is a long non-coding RNA transcribed on telomere repeats that increases in cells with short telomeres, and TERRA can sequester TRF2 from a gene regulated by the length of the distal telomere (Shay, 2018).

Telomeres play an essential role in the architectonics of the interphase nucleus (Figure 6).

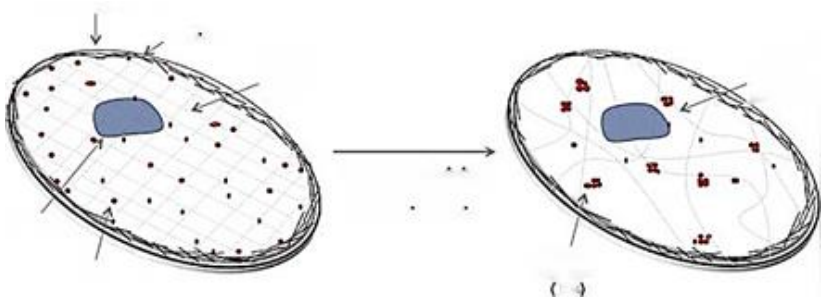

Fig. 6. Distribution of telomeres in the interphase nucleus

In normal cells (left), telomeres are scattered throughout the nucleus, with some telomeres showing preferential associations with the nuclear periphery or nucleolus. During oncogenic transformation, aging, or deregulation of lamins (proteins of the lamina underlying the inner membrane of the nuclear envelope), the distribution of telomeres changes, either increasing their connection with each other (telomere aggregates) or with the nuclear envelope (Novo, Londono-Vallejo, 2013).

Progeria – premature ging – is an example of a violation of the contacts of telomeres with progerin – lamine A. Mutated protein leads to an accelerated shortening of telomeres and premature aging (Rahman et al., 2021).

Even without mutations in lamina proteins there is a progressive shortening of telomeres with increasing age, which is associated with shifts in gene expression through changes such as the telomere position effect (TPE), suggesting a decrease in telomere interference with the transcriptional activity of more distant genes (Figure 7). Changes in telomeres positioning, because of shortening, affect the expression of a number of genes, so called telomere long distance effects

(TPE-OLD). This is why some genes far away from telomere (1-10 megabases, MB) are still affected by TPE, but genes closer to the telomere are not (Figure 7). With aging, shortening of telomere lengths lead to a change in the effect of gene expression (Zhang et al., 2021).

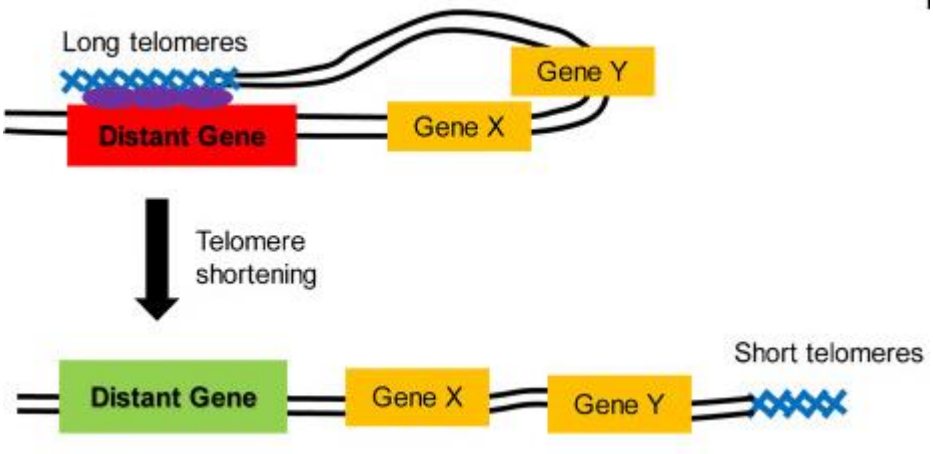

Fig. 7. Schematic of the distant effect of telomeric repeat shortening on gene distant expression (TPE-OLD)

Long telomeres can form a loop and interact with target genes that are far away. Red indicates inhibition of gene expression, green indicates an activated state. Other genes (yellow) in between are not affected. The distant interaction of the telomere and the gene can be mediated by the shelterin protein complex (purple) and weaken as the telomeres are shortened. Old cells, as a rule, have a smaller average telomere length (Zhang et al., 2021)

It should be noted that the telomerase, controlling the growth of telomeric repeats, is a specialized RNA-dependent DNA polymerase (reverse transcriptase). It means that telomeric repeats are evolutionary related with exogenous retroviruses, precursors of endogenous retrotransposons. The fact that telomeric repeats in Drosophila are represented by specific endogenous retroviruses further confirms this observation (Cacchione et al., 2020).

Centromeric regions of eukaryotic chromosomes contain another morphological element directly involved in the dynamics of the interphase nucleus architectonics (Liu et al., 2021; Bloom, Costanzo, 2017). In interphase nuclei centromeres form chromocenters, sometimes with tissue-specific dynamics. The small number of chromocenters is typical for rapidly dividing cells. There are many studies comparing the distributions of centromeres and chromocenters in animal and plant cells (Andrey et al., 2010). In one study, rabbit embryo cells, differentiated rabbit mammary gland epithelium cells during lactation, as well as differentiated cells of *Arabidopsis thaliana* were considered. The genomes of these species are significantly different. Rabbit genome has 44 chromosomes, while *A. thaliana* has only 10. Rabbit's genome size is 2.77 gigabases, while *A. thaliana* is 125 megabases. In *A. thaliana* differentiated cells, centromeres are grouped into chromocenters that are regularly distributed inside the nucleus. In rabbit's differentiated cells centromeres are also clustering more frequently as compared to embryonic cells. In the first prophase of meiosis, in wheat and mice, violations of the conjugation of homologous chromosomes are caused by mutations in orthologous genes. There is a high degree of homology between Ph1 and Cdk2 loci in mammals (Al-Kaff et al., 2008). The Cdk2 locus controls conjugation of homologs during meiosis in mice (Viera et al., 2009). Cdk2 is involved in initiating the onset of centrosome duplication (Schatten, 2008). Cdk2 is a part of the telomeric protein complex and prevents the fusion of sister chromatid telomeres (Konishi, de Lange, 2008).

The nucleotide sequence of centromeric regions is variable and consists of highly repeated tandem and dispersed repeats – minisatellites and mobile genetic elements (Balzano, Giunta, 2020). Thus, the eukaryotic genome, formed by linear chromosomes, is not only a symbiosis with archaeal and prokaryotic genomes, but also with mobile genetic elements that are presented, for example by retroelements, organizing telomeric and centromeric regions (Figure 8).

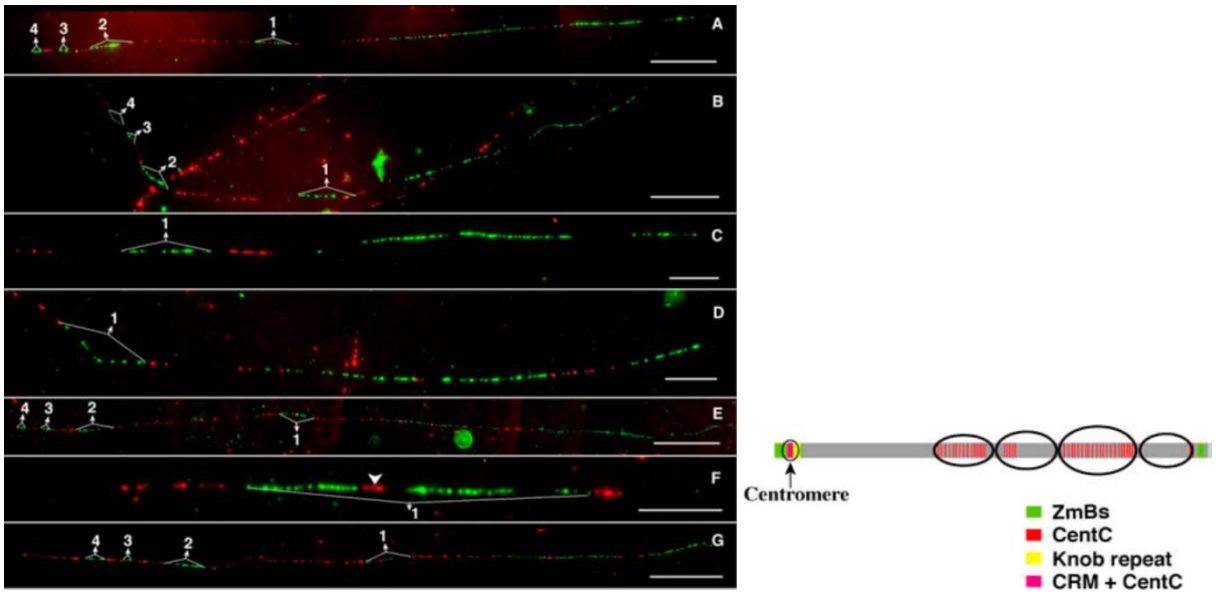

Fig. 8. The distribution of CentC repeats, retrotransposons CRM and ZmB in centromeric region of corn's chromosomes (Liu et al., 2020).

In several studies it was suggested that centromeres were derived from telomeres and the proof of concept was also provided (Villasante et al., 2007).

Thus, the formation of telomeres and centromeres, the two key elements of the interphase nucleus architectonics, is based on tandem repeats and exogenous retroviruses remnants. These genomic elements are closely related (Louzada et al., 2020). Those elements are prone to form secondary DNA structures, e.g. hairpins, quadruplex DNA structures, triplexes. Those structures may interfere with genome duplication, slowing down or even arresting replication fork, resulting in double strand breaks. Homological recombination can repair the breaks, but the presence of satellites and mobile genetic elements may lead to changes in nuclear architectonic and consequently gene expression programs. High recombination frequency between homological sequences of tandem repeats and transposable elements leads to the idea that these elements are an 'engine' promoting genome evolution. Genomic regions with these sequences are considered 'hot spots' for structural chromosome rearrangements, leading to species-specific changes in nuclear architectonic, creating new gene networks and gene expression programs.

Mammalian genomes are enriched with transposable elements (TE) (Percharde et al., 2020). There are not many DNA-transposons (< 3 %) and full-seized endogenous retroviruses (4-10 %), but the frequency of autonomous and non-autonomous retrotransposons is high.

Long interspersed repeated DNA LINE1 is the most successful TE family in terrestrial mammals (Percharde et al., 2020). Typical LINE1 family member is around 6,000 bp long and encode two proteins, ORF1 and ORF2, participating in transpositions. ORF1 is RNA-binding protein, ORF2 combines endonuclease (EN) and reverse transcriptase (RT) activities. Among ca 8868000 human and ca 599 000 mice LINE1 elements only 80-100 human LINE1 and 2300 mouse LINE1 still have transpositional activities in human and mouse genomes, respectively (Percharde et al., 2020).

LINE1 insertion happens mostly via endonuclease-dependent revers transcription. LINE1 RNA associates with several homotrimers of ORF1p and at least one dimer of ORF2p, forming ribonuclear protein RNP LINE1 in cytoplasm. RNP LINE1 then enters the nucleus where endonuclease ORF2p frees 3' hydroxyl group. This free 3' hydroxyl group then serves as a primer for cDNA LINE1 synthesis by reverse transcriptase ORF2p, starting from the polyA tail of mRNA LINE1. Short dispersed genomic element SINE also has polyA tail and it may compete with LINE1 polyA tail for LINE1 ORF2p reverse transcriptase, hijacking LINE1 transposition mechanism. Also LINE1 ORF2p can retrotranspose unique mRNA proteins and small nuclear RNAs (Percharde et al., 2020).

LINE1 retrotranspositions depend on other cellular proteins. There are positive regulators of transpositions, in particular nucleolin and heterogeneous nuclear riboproteins (hnRNPs), mitogen

activated proteinkinases and cyclin-dependent kinases. DNA repair mechanism concludes LINE1 insertion. Mammalian genomes have several mechanisms at transcriptional, post-transcriptional and posttranslational levels, restricting LINE1 transposition. CpG DNA methylation and histone modifications at the LINE1 promoter can limit LINE1 transcription. KRAB-ZFP proteins (zinc finger proteins with DNA interacting motif) specifically recognize ERV and LINE1 and attract KAP1 (heterochromatin protein). Posttranscriptional repression LINE1 RNA occurs through RNA-interference with small RNAs. LINE1 retrotransposition can also be restricted at the posttranslational level with interferon-induced genes (Percharde et al., 2020).

New LINE1 insertions happens approximately 1 in 100 human births and 1 in 8 mouse births. LINE1 interferes with genome homeostasis in many ways, in particular: i) LINE1 activity induces genome insertions; ii) LINE1 activity influence SINE/Alu retrotranspositions, which are also involved in genomic instability; iii) LINE1 ORF2 endonuclease activity may have some mutagenic effects independently on retrotransposition; iv) LINE1 and SINE elements may influence short tandem genome-abundant AT-rich repeat; v) repetitive property LINE1 and SINE elements can induce large-scale genomic rearrangements, such as inversions and duplications. On the average, any two haploid human genomes have approximately one thousand different TE insertions, mostly from LINE1 and Alu families (Percharde et al., 2020).

LINE1 family high frequency in mammalian genomes positions these elements to play a central role in local chromatin organization and, further, higher level chromatin architecture. LINE1 and SINE elements, both depending on LINE1 ORF2 activity for transposition, have very different genomic distribution. LINE1 are frequent in gene poor, AT-rich heterochromatin regions while SINE elements are frequent in gene rich, GC-rich, euchromatin regions. In interphase nucleus there is similar subdivision between compartments: (B) – silence and (A) – expression. It is highly probable that LINE1 and SINE elements not only correlate with B and A compartments, respectively, but also can participate in formation of chromosomal domains in these two compartments. The high association of RNA repetitive sequences, including LINE1 RNA, with chromatin, and evidence that chromatin-bound RNA contributes to the global organization of chromatin, supports this hypothesis.

TEs such as LINE1 and various endogenous retroviruses (ERVs) become globally demethylated and expressed during major epigenetic reprogramming in the germline. This erasure of epigenetic memory occurs naturally *in vivo* in the course of normal embryonic development. Similarly, TE de-repression via H3K9me2 happens in induced pluripotent stem cells. Many TE families have cis-regulatory activity. Gradually it is becoming clear that transcribed TE genes are also important in early development. Transcribed HERVH RNA is important to maintain human embryonic stem cells (ESC) in non-differentiated state, presumably acting as lncRNAs. HERVK encoded protein Rec is highly expressed in human embryos increasing antiviral resistance by increasing IFITM1 proteins regulation. Rec also binds a subset of endogenous RNAs regulating they ribosome coverage and expression the way that can be important for early human development.

Actually, the relationship between many TEs and pathways limiting their mutagenic activity can be considered in terms of the balance between beneficial and negative functions of TE. The involvement of TE expression in the early stages of growth and development, increased genetic and epigenetic variability, thus providing an adaptation mechanism in ever-changing environment, are both beneficial TE functions. However, this metastable state of TEs in some cases results in a disease, if retrotransposition event goes wrong. In other words, potential reactivation of TEs in adult somatic cells and their association with diseases such as cancer may be the price to pay for their role in development and evolution (Percharde et al., 2020).

Many studies confirm that tandem and dispersed repeats are involved in the regulation of changes in gene expression programs through dynamic changes in interphase nucleus architectonics. The most appealing example is the work performed on the interphase nuclei of cylindrical photoreceptor cells of nocturnal mammals, where an inverted pattern of heterochromatin and euchromatin distribution, in comparison with other nuclei, was observed. Heterochromatin was located inside, euchromatin – on the periphery of the nucleus under the lamina (Figure 9) (Falk et al., 2019). The authors of this study came to the conclusion that, in particular, ectopic contacts between homologous dispersed repeats localized in different regions of chromatin can make a significant contribution to such an inverted variant.

Redistributions of hetero- and euchromatin have been described in rabbit embryos starting from the four cells stage (Bonnet-Garnier et al., 2018).

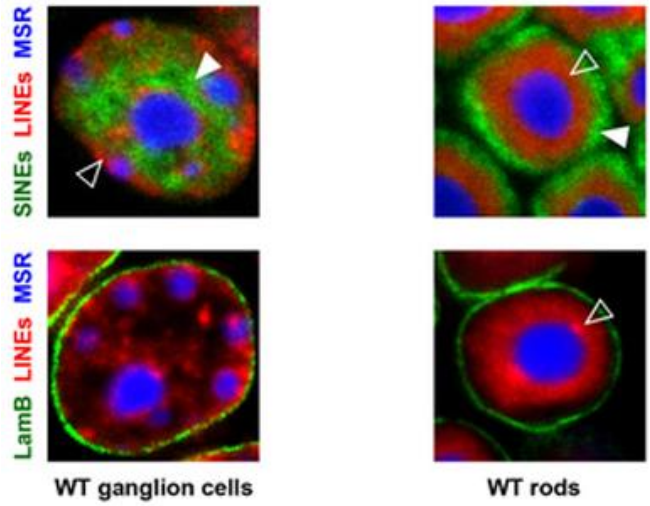

Fig. 9. The distribution of heterochromatin markers LINE (red), euchromatin marker SINE - green and MSR - microsatellite sequences in the nuclei of ganglion cells (left) and cylindrical photoreceptor cells (right) (Falk et al., 2019).

The significant importance of interchromosomal interactions is in a good agreement with our earlier data on two main types of chromatin contacts in the space of the interphase nucleus - with the periphery of the nucleus and between chromosomes (Figure 10).

Fig. 10. Contacts variants of 4 polytene chromosomes in the saliva gland of the *Chironomus thummi* larva after centrifugation

Chromosomes form long strands attached to the periphery of the nucleus; Tight interchromosomal contacts with each other; a - chromosome 4, bearing the nucleolus, maintaining contact with the periphery of the nucleus (40×12.5) (Glazko, Zayniev, 1986).

It should be noted that DNA copies of exogenous retroviruses – precursors to a certain retrotransposons, as a rule, are localized in the regions of genomes where matrix attachment regions (MAR) are found (Johnson, Levy, 2005; Narwade et al., 2019).

There is a lot of data showing that reproductive barriers can form even between closely related animals, for example, between subspecies of the European rabbit (Carneiro et al., 2014), TE activation during hybridization, leading to reproductivity reduction (Laporte et al., 2019), or genomic rearrangements and the appearance of new species (Auvinet et al., 2018). Now, the importance of these data is as high as ever, because of climate changes, farm animals' transportation to new ecological and geographic regions, as well as genetic erosion of factory breeds. All of the aforementioned factors require an increase in the adaptive potential of animals, that can be achieved by hybridization with closely related wild species (for example, (Cao et al.,

2021)). This is obviously hindered by the high rate of transposons evolution, which is involved in genetic divergence, in particular, of centromeric sequences, contributing to the errors during mitosis and meiosis, and a reduction of hybrid animals' reproduction.

Evolutionary rate of transposons is the best to evaluate using their spectral differences in laboratory strains of mice, created no more than 100 years ago (Nellaker et al., 2012). Transposons-based dendrogram corresponds to the history of genetically defined lines breeding (Figure 11).

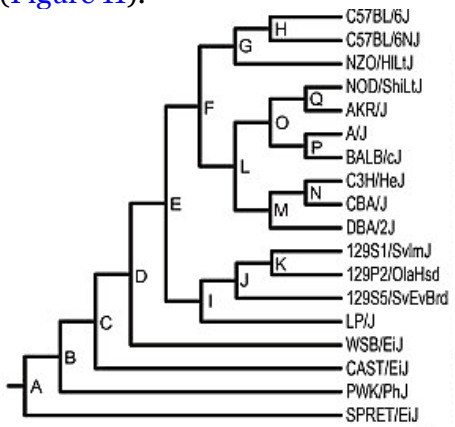

Fig. 11. Dendrogram of genetic relationships between laboratory strains of mice, built on the basis of the presence/absence of homological sites in different retrotransposons (Nellaker et al., 2012)

In our own research, while we were analyzing the metaphase plates of the cell populations from fusion of mouse and mink cells, we found an explanation for the high rate of mink's chhromosome loss in those cell hybridomas. Simply, mink chromosomes were not able to attach to the division spindle (Figure 12).

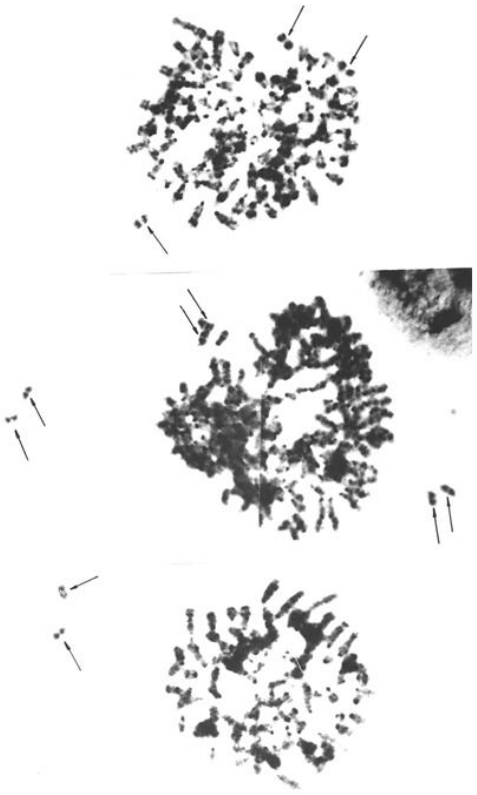

Fig. 12. Metaphase plates of mouse-mink hybridomas. Arrows indicate mink chromosomes located outside the boundaries of the mouse chromosome accumulation (Glazko, 1988)

In early 1980 Michael Bennett had shown, for hybrid plants, that there is a specificity of chromosomal sets interactions with division spindle. Haploid sets in hybrides were clearly separated (Figure 13).

Fig. 13. Metaphase plates of burley and wild rye hybrids. After FISH hybridization 7 barley chromosomes (orange) are surrounded by 7 wild rye chromosomes (yellow) (Leitch et al., 1990)

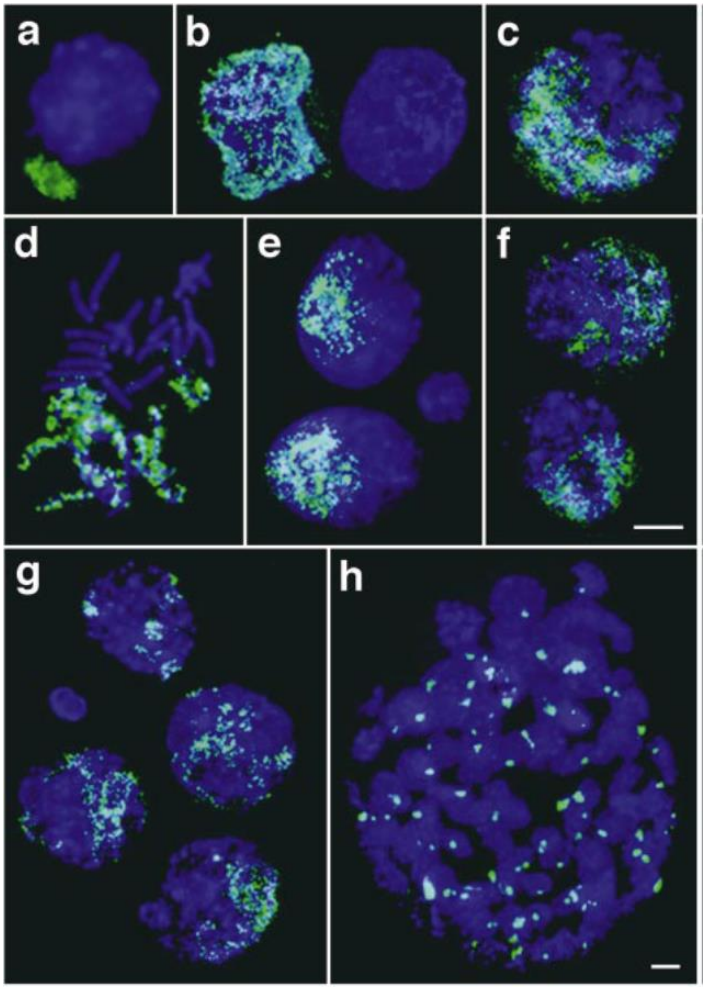

Fig. 14. Distribution of paternal chromatin in early mouse embryos (Mayer et al., 2000)

In plants, similar to mammalian hybrids (Figure 12), one species is losing chromosomal set faster than the other (Polgari et al., 2019).

Interestingly enough, starting from zygotic phase in mammalian cells there is spatial separation between diploid and haploid chromosomal sets (Figures 14, 15).

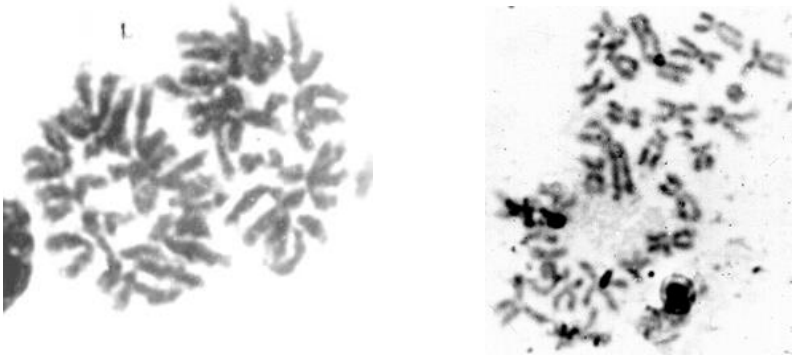

Fig. 15. Separation into haploid chromosomal sets in bone marrow cells of *Mus musculus* end *Microtus oeconomus*

As it was already mentioned, tandem and dispersed repeats are directly involved in the architectonics of the interphase nucleus, providing ectopic contacts between chromosomes and between chromosomal centromeric regions (Figures 16, 17).

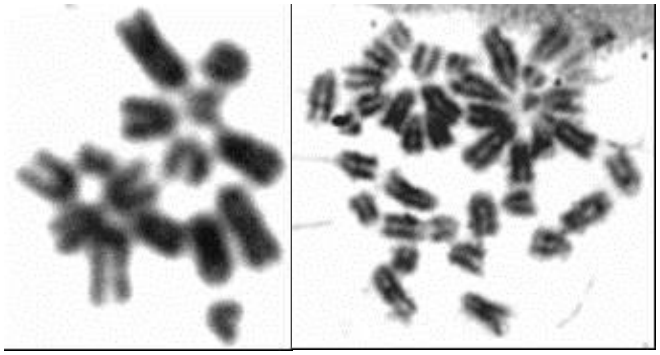

Fig. 16. Centromeric contacts between non-homologous chromosomes in the cell population of G1 embryonic stem cells from embryonic fibroblasts BALB/c mice strain

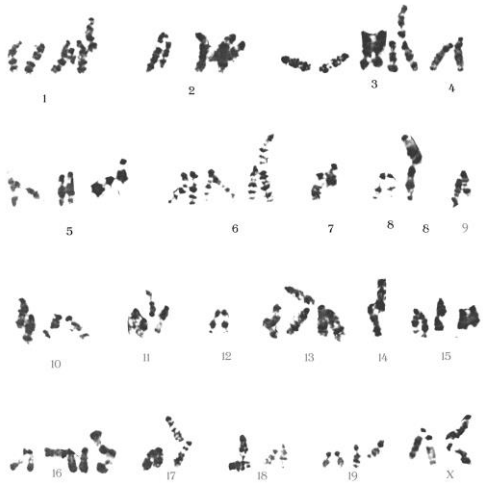

Fig. 17. Ectopic contacts between homologous chromosomes in metaphase plates of the FC3H8 line – embryonic fibroblasts of the laboratory line of C3H mice. The numbers indicate the numbers of the chromosomes entering into associations. Associations of both two and three homologous chromosomes are shown

It is interesting to note that in the cells of the bone marrow of highly inbred laboratory mice strain there is non-homologous chromosomes clustering in centromeric regions (Figure 18A). Such clustering can become Robertsonian translocations when mice are injected with the inducer of single-strand breaks adriamycin (Figure 18B).

A B

Fig. 18. A. Centromeres clustering of non-homologous chromosomes in bone marrow cells of BALB/c laboratory mice; B. Robertsonian translocations formation in mice of the same strain after administration of the inducer of single-strand breaks adriamycin. The arrow indicates the Robertsonian translocation between chromosomes 1; 8

In our previous studies, we compared genomic elements flanked by inverted repeats of microsatellites, in particular with core motif AGC, in Holstein cattle infected with bovine leukemia retrovirus and infection-free animals. We found that infected animals had higher density of retrotransposons and their recombination products as compared to infection-free animals (Glazko et al., 2018). This result suggests that individual differences in retroviral infection resistance could be related, to some extent, with genomic 'resistance' to mobile genetic elements insertions and deletions.

Actually this hypothesis was confirmed with data, accumulated during the aftermath of COVID-19 pandemic. COVID-10 did induce retrotransposons expression in lung and intestine cells. The authors of those studies suggest that retrontransposons activation lead to genomic instability and enhance genes expression, in particularly, reverse transcriptase gene. Therefore people with high basal rate of transposons activity, such as elderly and cancer patients, may have higher risk of additional retrotransposons' activation. Long-term epigenetic inheritance of retrotransposons' activity is now proven. Chimeric transcripts of transposons' RNA and SARS-CoV-2 RNA were also recently found, suggesting potential insertions viral fragments in human genome. Most frequently, chimeric RNA was composed from leading and terminal fragments of SARS-CoV-2 genome. Those findings demonstrate that coronavirus invades human cells and interacts with transposons, leading to more severe disease trajectory in vulnerable patients (Cohen, 2021).

4. Conclusion

Interphase nucleus architectonic and its dynamic have leading role in changing and regulating gene expression programs. In particular, it is achieved through chromatin packaging and positioning, regulating nucleotide sequences methylation and demethylation. Chromatin's architectonic is changing by employing two leading elements: ectopic inter-chromosomal contacts as well as telomeres and centromeres. The major part of centromeres and telomeres consist of tandem repeats and retrotransposons. Around half of mammalian genomes, is made out of transposons (mostly retrotransposons) and their recombination products. These elements have high evolutionary rate and even individual variability is influencing phenotypic variability and reproductive rate of plants and animals. Different interactions of *caryoskeleton's elements, such as SINEs and LINEs, with heterochromatin and euchromatin genomic domains, their movements inside the nucleus' space, could be related with gene clusters expressed at different levels.* It is expected that low genomic 'resistance' toward exogenous retroviruses and retrotranspositions is

controlled by natural selection and significantly influence population genetic dynamic in generations and the appearance of new forms.

References

Al-Kaff et al., 2008 – *Al-Kaff, N., Knight, E., Bertin, I. et al.* (2008). Detailed dissection of the chromosomal region containing the Ph1 locus in wheat Triticum aestivum: with deletion mutants and expression profiling. *Ann Bot*. 101: 863-872.

Andrey et al., 2010 – *Andrey, P., Kieu, K., Kress, C., et al.* (2010). Statistical analysis of 3D images detects regular spatial distributions of centromeres and chromocenters in animal and plant nuclei. *PLoS Comput Biol*. 6: e1000853.

Auvinet et al., 2018 – *Auvinet, J., Graca, P., Belkadi, L. et al.* (2018). Mobilization of retrotransposons as a cause of chromosomal diversification and rapid speciation: the case for the Antarctic teleost genus Trematomus. *BMC Genomics*. 19: 339.

Balzano and Giunta, 2020 – *Balzano, E. and Giunta, S.* (2020). Centromeres under Pressure: Evolutionary Innovation in Conflict with Conserved Function. *Genes (Basel)*. 11.

Bloom and Costanzo, 2017 – Bloom, K. and Costanzo, V. (2017). Centromere Structure and Function. *Prog Mol Subcell Biol* 56: 515-539.

Bonnet-Garnier et al. 2018 – *Bonnet-Garnier, A., Kieu, K., Aguirre-Lavin, T., et al.* (2018). Three-dimensional analysis of nuclear heterochromatin distribution during early development in the rabbit. *Chromosoma*. 127: 387-403.

Cacchione et al., 2020 – *Cacchione, S., Cenci, G. and Raffa, G.D.* (2020). Silence at the End: How Drosophila Regulates Expression and Transposition of Telomeric Retroelements. *J Mol Biol*. 432: 4305-4321.

Cao, et al. 2021 – *Cao, Y.H., Xu, S.S., Shen, M,, et al.* (2021). Historical Introgression from Wild Relatives Enhanced Climatic Adaptation and Resistance to Pneumonia in Sheep. *Mol Biol Evol*. 38: 838-855.

Carneiro, M. et al., 2014 – *Carneiro, M., Albert, F.W., Afonso, S., et al.* (2014). The genomic architecture of population divergence between subspecies of the European rabbit. *PLoS Genet*. 10: e1003519.

Cohen, 2021 – *Cohen, J.* (2021). Do coronavirus genes slip into human chromosomes? *Science*. 372: 674-675.

Cui et al., 2020 – *Cui, T., Li, Z., Zhou, Q., et al.* (2020). Current advances in haploid stem cells. *Protein Cell*. 11: 23-33.

Deakin et al., 2019 – *Deakin, J.E., Potter, S., O'Neill, R., et al.* (2019). Chromosomics: Bridging the Gap between Genomes and Chromosomes. *Genes (Basel)*. 10.

Falk et al., 2019 – *Falk, M., Feodorova, Y., Naumova, N., et al.* (2019). Heterochromatin drives compartmentalization of inverted and conventional nuclei. *Nature*. 570: 395-399.

Fritz et al., 2019 – *Fritz, A.J., Sehgal, N., Pliss, A., et al.* (2019). Chromosome territories and the global regulation of the genome. *Genes Chromosomes Cancer*. 58: 407-426.

Glazko 1988 – *Glazko, T.T.* (1988). Karyotypic characteristicsof a number of clonal lines of an interspecificmouse-mink hybridoma. *Tsitologia Russian)*. 30: 597-605.

Glazko and Zayniev, 1986 – *Glazko, T.T. and Zayniev, G.A.* (1986). Heterogrnrity changes of morphologyof nuclei in salivaryglands of larva of *Chironomus thummi* during centrifugation. *Tsitologiya (Russian)*. 28: 920-927.

Glazko et al., 2018 – *Glazko, V., Kosovsky, G. and Glazko, T.* (2018). High Density of Transposable Elements in Sequenced Sequences in Cattle Genomes, Associated With AGC Microsatellites . *Glo. Adv. Res. J. Agric. Sci.* 7(2): 034-045. 7: 034-045.

Johnson and Levy, 2005 – Johnson, C.N. and Levy, L.S. (2005). Matrix attachment regions as targets for retroviral integration. *Virol J*. 2: 68.

Konishi and de Lange, 2008 – *Konishi, A. and de Lange, T.* (2008). Cell cycle control of telomere protection and NHEJ revealed by a ts mutation in the DNA-binding domain of TRF2. *Genes Dev*. 22: 1221-1230.

Laporte et al., 2019 – *Laporte, M., Le Luyer, J., Rougeux, C., et al.* (2019). DNA methylation reprogramming, TE derepression, and postzygotic isolation of nascent animal species. *Sci Adv*. 5: eaaw1644.

Leitch et al., 1990 – *Leitch, A.R., Mosgoller, W., Schwarzacher, T., et al.* (1990). Genomic in situ hybridization to sectioned nuclei shows chromosome domains in grass hybrids. *J Cell Sci.* 9(Pt 3): 335-341.

Li et al., 2014 – *Li, W., Li, X., Li, T., et al.* (2014). Genetic modification and screening in rat using haploid embryonic stem cells. *Cell Stem Cell.* 14: 404-414.

Liu et al., 2021 – *Liu, Q., Liu, Y., Shi, Q., et al.* (2021). Emerging roles of centromeric RNAs in centromere formation and function. *Genes Genomics.* 43: 217-226.

Liu et al., 2020 – *Liu, Y., Su, H., Zhang, J., et al.* (2020). Back-spliced RNA from retrotransposon binds to centromere and regulates centromeric chromatin loops in maize. *PLoS Biol.* 18: e3000582.

Louzada et al., 2020 – *Louzada. S., Lopes. M., Ferreira. D., et al.* (2020). Decoding the Role of Satellite DNA in Genome Architecture and Plasticity-An Evolutionary and Clinical Affair. *Genes (Basel).* 11.

Mayer et al., 2000 – *Mayer, W., Smith, A., Fundele, R., et al.* (2000). Spatial separation of parental genomes in preimplantation mouse embryos. *J Cell Biol.* 148: 629-634.

Narwade et al., 2019 – *Narwade, N., Patel, S., Alam, A., et al.* (2019). Mapping of scaffold/matrix attachment regions in human genome: a data mining exercise. *Nucleic Acids Res.* 47: 7247-7261.

Nellaker et al., 2012 – *Nellaker, C., Keane, T.M., Yalcin, B., et al.* (2012). The genomic landscape shaped by selection on transposable elements across 18 mouse strains. *Genome Biol.* 13: R45.

Novo and Londono-Vallejo, 2013 – *Novo, C.L. and Londono-Vallejo, J.A.* (2013.) Telomeres and the nucleus. *Semin Cancer Biol.* 23: 116-124.

Percharde et al., 2020 – *Percharde, M., Sultana, T. and Ramalho-Santos, M.* (2020). What Doesn't Kill You Makes You Stronger: Transposons as Dual Players in Chromatin Regulation and Genomic Variation. *Bioessays* 42: e1900232.

Polgari et al., 2019 – *Polgari, D., Mihok, E. and Sagi, L.* (2019). Composition and random elimination of paternal chromosomes in a large population of wheat x barley (*Triticum aestivum L.* × *Hordeum vulgare* L.) hybrids. *Plant Cell Rep.* 38: 767-775.

Rahman et al., 2021 – *Rahman, M.M., Ferdou,s K.S., Ahmed, M., et al.* (2021). Hutchinson-Gilford Progeria Syndrome: An Overview of the Molecular Mechanism, Pathophysiology and Therapeutic Approach. *Curr Gene Ther.* 21: 216-229.

Schatten, 2008 – *Schatten, H.* (2008). The mammalian centrosome and its functional significance. *Histochem Cell Biol.* 129: 667-686.

Shay, 2018 – *Shay, J.W.* (2018). Telomeres and aging. *Curr Opin Cell Biol* 52: 1-7.

Viera et al., 2009 – *Viera, A., Rufas, J.S., Martinez, I., et al.* (2009). CDK2 is required for proper homologous pairing, recombination and sex-body formation during male mouse meiosis. *J Cell Sci.* 122: 2149-2159.

Villasante et al., 2007 – *Villasante, A. Abad, J.P. and Mendez-Lago, M.* (2007). Centromeres were derived from telomeres during the evolution of the eukaryotic chromosome. *Proc Natl Acad Sci U S A.* 104: 10542-10547.

Zhang et al., 2021 – *Zhang, N., Li, Y., Lai, T.P., et al.* (2021). Imaging assay to probe the role of telomere length shortening on telomere-gene interactions in single cells. *Chromosoma.* 130: 61-73.

Published in the USA
Biogeosystem Technique
Issued since 2014.
E-ISSN: 2413-7316
2022. 9(2): 77-88

DOI: 10.13187/bgt.2022.2.77
https://bgt.cherkasgu.press

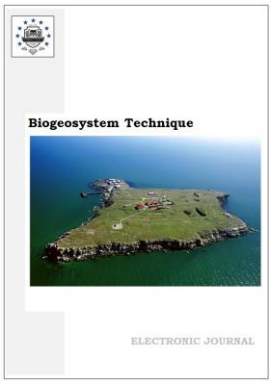

Comparative Case Study of Atmospheric Parameters over India and China during Covid 19 Lockdown

Abhishek Singh [a, *], Sapna Rawat [b], Anil Kumar Singh [c], Karen Ghazaryan [a], Omkar Singh [d], Ragini Sharma [e], Neha Chakrawarti [f], Sakshi Singh [g], Omkar Singh [h]

[a] Faculty of Biology, Yerevan State University, Yerevan, Armenia
[b] Department of Botany, University of Delhi, India
[c] University of Allahabad, Senate House Campus, University Road, Old Katra, Prayagraj (Allahabad), Uttar Pradesh, India
[d] ICAR-Indian Institute of Farming Systems Research, Meerut, U.P., India
[e] Department of Genetics and Plant breeding, Govind Ballabh Pant University of Agriculture and Technology, Pant-Nagar, India
[f] Punjab Agricultural University, Ludhiana, Punjab, India
[g] T.D, P.G Collage, Jaunpur, Uttar Pradesh, India
[h] ICAR-Krishi Vigyan Kendra, PG College Ghazipur-233001 (UP), India

Paper Review Summary:
Received: 2022, November 25
Received in revised form: 2022, December 8
Acceptance: 2022, December 16

Abstract

The novel coronavirus disease (Covid-19) was first reported in China on December 8, 2019, and in India on January 27, 2020, as per the World Health Organization (WHO). Government of India and China implemented rapid and stringent measures to contain the spread of COVID-19, which included lockdowns and restrictions on population's mobility. This study aims to investigate concentrations of NO_2 emission, stratospheric ozone status, and temperature before and during the lockdown in India and China. In India lockdown was implemented from March 22 to May 31 and in China from January 23 to April 8, 2020. NO_2 concentration, stratospheric ozone, and temperature of 2019 and 2020 were compared in both countries during the study period (January 1 – May 31). Our results showed a significant reduction in NO_2 concentration up to 4-16 % and 4-40 % over India and China respectively, during the lockdown period. We observed a similar percentage change in concentration of stratospheric ozone was 1-12 % in India as well as China. Similarly, the percentage reduction in temperature was 0-5 % and 1-94 % in India and China respectively. Further analysis of satellite data revealed that NO_2 emission decreased in April and May 2020 in India and from January to May 2020 in China. The study also showed a positive effect of lockdown on stratospheric ozone concentration, which increased during entire study period from January to May 2020 compared to 2019. While the COVID-19 lockdown had severe social and economic impacts, it positively impacted the natural environment.

* Corresponding author
E-mail addresses: intmsc.abhi@gmail.com (A. Singh), singhanil854@gmail.com (A. Kumar Singh)

Keywords: Covid-19, NO_2, stratospheric ozone, temperature, Sentinel-5P satellite

1. Introduction

China notified WHO (World Health Organization) about several unusual pneumonia cases in Wuhan, a city in the central Hubei Province, in December (Gautam, Hens, 2020). It was identified as a new virus named SARS-CoV-2 and was announced by WHO (WHO, 2020a) on 7 January 2020. WHO declared a worldwide emergency for public health. China's government imposed a lockdown in Wuhan and other cities in Hubei to quarantine the center of COVID-19 outbreaks on 23 January 2020, commonly known as the Wuhan lockdown. The recent outbreak of corona virus disease has raised global concerns and led to total lockdowns in many countries. At the end of January 2020 and the beginning of February 2020, the situation in many countries such as Iran, Italy, etc., became terrifying and the number of deaths started increasing day by day. Starting in March 2020, the epidemic disease turned into a pandemic condition. By the end of March 2020, half of the world's population was undergoing different lockdowns (Muhammad et al., 2020). COVID-19 is a contagious disease caused by severe acute respiratory syndrome coronavirus 2 (SARS-CoV-2) (WHO 2020a; Wang et al., 2020) and has an approximate fatality rate of 2-3 % (Rodriguez Morales et al., 2020). This virus can spread from infected people to non-infected people (Bherwani et al., 2020). The spread of the virus can be limited by wearing masks, maintaining social distancing, avoiding public gatherings and avoiding the use of public transport, etc, which have a high risk of virus contamination and spreading (WHO, 2020b; Bherwani et al., 2020; Gautam, 2020). To control the spread of COVID-19 various countries such as China and the Indian government announced a series of lockdowns from 23 January in China (BBC, 2020) and 24 March 2020 in India (Regen et al., 2020), which included closing schools, universities, restricting transportation and the movement of people between provinces. The economy of countries was affected negatively due to the COVID-19 lockdown, and also a severe decline in economic development due to restriction movement and transportation to control the spread of the virus. Due to a reduction in economic activities and vehicular transport, air pollution was also reduced (Wang and Su, 2020). That lead to considerable improvement in air quality in various countries such as Spain (Tobías et al., 2020), India (Gautam, 2020), Brazil (Nakada, Urban, 2020), and China (Sharma et al., 2020). The concentration of pollutants was also decreased obviously due to restrictions in anthropogenic activities. Air is a vital element for the survival of living beings, so it is necessary to keep it clean, pollutant-free, and safe to breathe. Due to various anthropogenic activities, air quality is decreasing leading to emission of harmful gases and air pollutants in higher concentration, which can damage the health of all living beings (Gautam, Hens, 2020a). The major air pollutants are particulate matter (PM), sulfur dioxide (SO_2), nitrogen dioxide (NO_2), ozone (O_3), carbon monoxide (CO), and carbon dioxide (CO_2) (Chen et al., 2007). NO_2 is one of the major air pollutants and also a precursor of ground-level tropospheric ozone, particulate matter, and acid rain (Bechle et al., 2013). It is emitted during the process of combustion of fossil fuels and transportation (Muhammad et al., 2020). In most of the regions with the increase in NO_2 concentration, O_3 declines as in urban-dominated regions, while the decline in NO_2 emission leads to an increase in O_3 as in rural areas (Dentener et al., 2020). The changes in NO_2 concentration in this lockdown period can provide an understanding into the achievability of air quality improvement when there were restrictions in emissions of harmful gases from anthropogenic activities and gives better regulatory plans to control air pollution. In this paper, we analyzed the variations in sentinel satellite data of ground-based NO_2 concentration, ozone and temperature from two countries i.e., China and India for the two past years (2019-2020) from January 1st to May 31st. Comparison of data in the last two years aids in understanding the potential effect of change in gaseous emissions during days with similar meteorology. The objective is to evaluate the relative variation in NO_2 emission and ozone concentration before and during the lockdown period to evaluate the impacts of COVID-19 lockdown conditions on the air quality of India and China.

2. Material and methods

2.1. Site description

India is the second most populated country in the world after China. The countries selected for the present study include India and China. India and China are parts of the Asia continent and are neighboring countries. India is situated north of the equator between 8°4′ north to 37°6′ north

latitude and 68°7′ east to 97°25′ east longitude and occupies 3,286,927 km² areas. China occupies approx. 9,596,960 km² area located in the southeast region of the Asia continent.

2.2. Datasets

2.2.1. Sentinel-5P data

TROPOMI is a passive-sensing hyperspectral nadir-viewing imager onboard Sentinel-5 Precursor (S-5P) satellite, launched on October 13, 2017. The S-5P is a near-polar sun-synchronous orbit satellite flying at a height of 817 km, with an overpass local time at ascending node (LTAN) of 13:30 and a repeat cycle of 17 d (KNMI, 2017). The TROPOMI works in a non-filtering push broom setup, with an instantaneous field of view of 108◦ and an estimated time of around 1s. The outcome is an area with width approximately 2600 km, an along-track goal of 7 km, and day by day worldwide inclusion (KNMI, 2017). It has four separate spectrometers, measuring the ultraviolet (UV), UV–visible (UV-VIS), near-infrared (NIR), and short-wavelength infrared (SWIR) spectral bands, of which the NIR and SWIR bands are new compared to its predecessor OMI (Veefkind et al., 2012). The NO_2 sections are inferred utilizing TROPOMI's UV–VIS spectrometer backscattered sunlight-based radiation estimations in the 405–465 nm frequency range (van Geffen et al., 2015; van Geffen et al., 2019). The swath area is partitioned into 450 individual valuation pixels, which bring about a close nadir resolution of 7×3.5 km. The total NO_2 slant column density is retrieved from Level 1b UV–VIS radiance and solar irradiance spectra utilizing the DOAS strategy (Platt and Stutz, 2008). The NO_2 retrieval and assimilation scheme and the data product have been described in detail (Eskes et al., 2019; van Geffen et al., 2015; van Geffen et al., 2019; Veefkind et al., 2012). The TROPOMI NO_2 processing system is based on the algorithm developments for the DOMINO-2 product and for the EU QA4ECV NO_2 reprocessed dataset for OMI and has been adopted for TROPOMI. The Assimilation-modelling system uses the 3-dimensional global TM5-MP chemistry transport model at a resolution of a 1x1 degree as an essential element. In this research, near real-time NO_2 concentrations images were created using the google earth engine. These images were pre-processed, corrected, and stored in the google earth engine database.

2.2.2. CFSR

The Climate Forecast System, NCEP version 2 (CFSv2) is an upgraded version of CFS version 1 (CFSv1). It is a reanalysis product first developed as part of the Climate Forecast System by NCEP in 2004 with quasi-global coverage and is a fully coupled atmosphere-ocean–land model used by NCEP for seasonal prediction (Saha et al., 2014). CFSR has a 3D variational analysis scheme of the upper-air atmospheric state with 64 vertical levels and a horizontal resolution of 38 km spanning the period 1 January 1979 to the present day (Saha et al., 2014).

2.2.3. Analysis of data

Statistical analysis of data was performed using Microsoft Excel. Two-tailed Student' t-statistic was applied to the data of 2019 and 2020. The study revealed a significant difference ($p<0.05$) in NO_2 concentration between both the year's understudy with the confidence of 95 %. Descriptive statistical analysis of the data (for 2019 and 2020) was carried out for the calculation of mean and standard deviation.

3. Result and discussion

3.1. NO_2 level in India

The data presented in figure 1 depicts the NO_2 concentration (mol/km²) in India, before (1 January to 21 March 2020) and during the lockdown (22 March to 31 May 2020). The average concentration of NO_2 in India varied between 61-77 and 62-68 mol/km² during the study period 2019 and 2020 respectively. A major significant reduction was found in the NO_2 concentration level ($P < 0.005$). The highest reduction was found on April 1 to 10 April 2020 with respect to 2019 in the same period was 16% (Figure 2). However, the average reduction varied between 1-16 % during the entire study period. The marked reduction was observed in NO_2 level in India during the lockdown period (22 March to 31 May 2020) i.e., 4-16 % (Figure 2). Similarly, the corresponding decrease before the period of lockdown (1 January to 21 March) was 1-13 %. This reduction in NO2 concentration during the lockdown period was attributed to the decreased vehicular movement (Figures 1, 2).

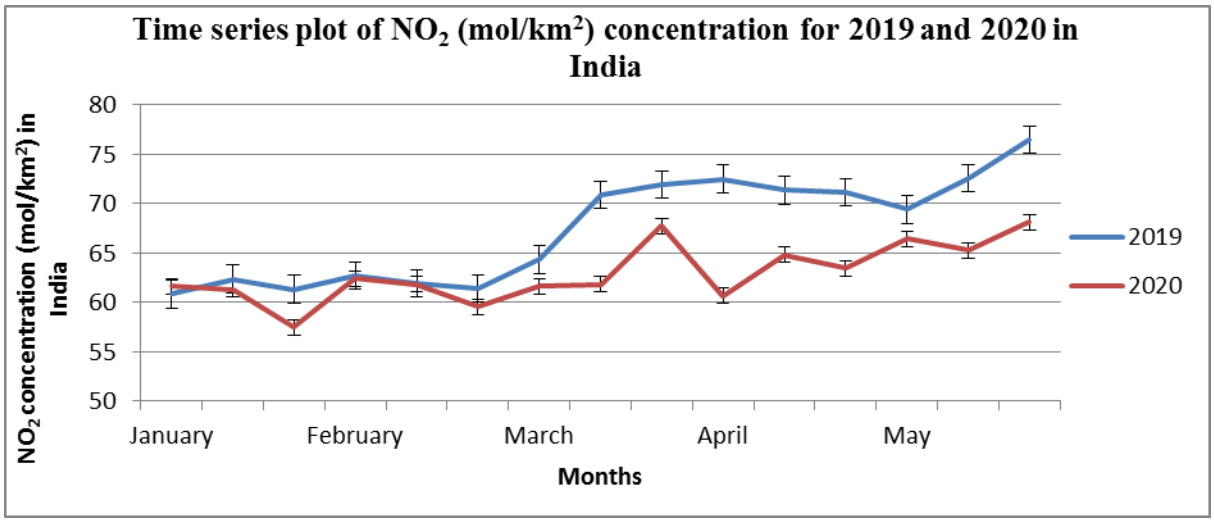

Fig. 1. NO_2 concentration (mol/km²) for the year 2019 and 2020 in India

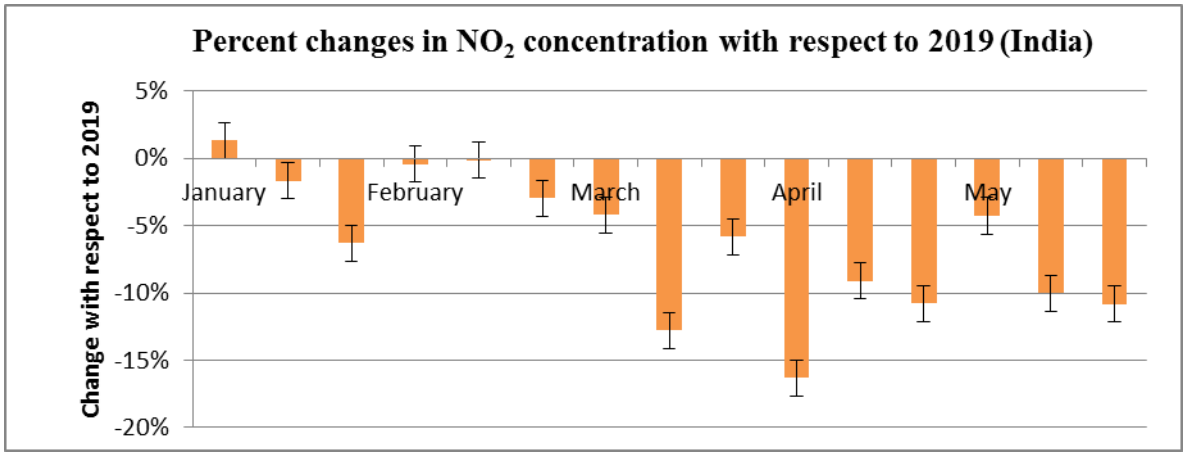

Fig. 2. Total percentage change in NO_2 level of the year 2020 (Jan-May) with respect to 2019

3.2. Ozone (stratospheric) in India

In India, there was a significant increase in Ozone level (mol/m²), which was considerably higher in 2020 compared to 2019 in India. The average ozone concentration during the study period varied between 0.107-124 and 116-130 in the study period of 2019 and 2020 respectively (Figure 3). A significant increase was found in Ozone level ($P < 0.005$) in 2020 as compared to 2019 across India. The average increase in Ozone concentration varied between 1-12 % (Figure 4) with respect to 2019 in the study period. The marked highest increase was observed from April 1 to April 10, 2020 (12 %). The percent increment in the lockdown period was 1 to 12 % with respect to 2019 in the same period (Figure 4). The increase in ozone levels in India was associated with a decrease in NO2 levels, as they have an inverse relationship.

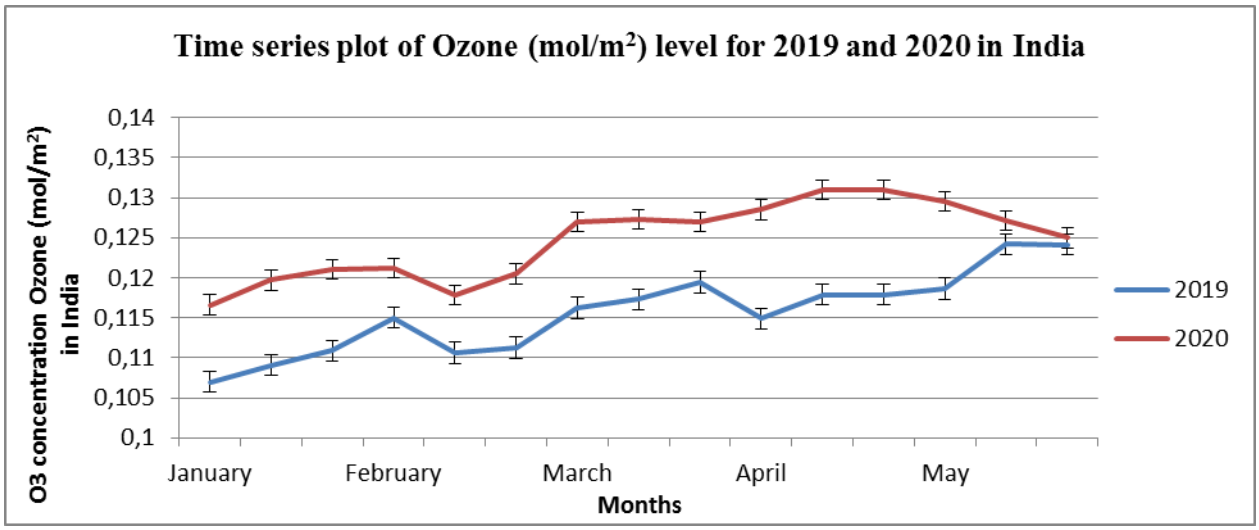

Fig 3. Time series plot of Ozone (mol/m²) level for 2019 and 2020 in India

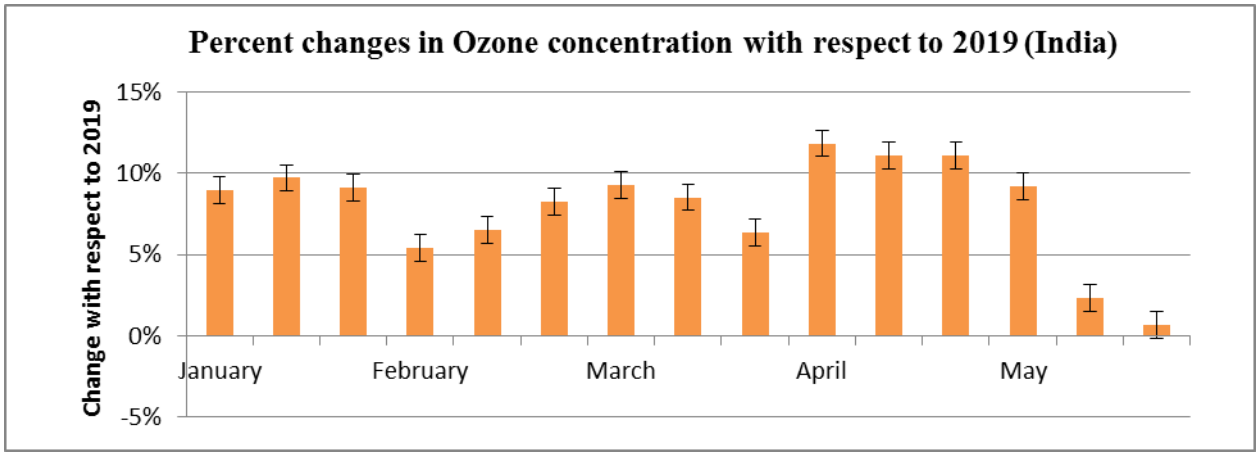

Fig 4. Total percentage change in Ozone level of the year 2020 (Jan- May) with respect to 2019

3.3. Temperature in India

The temperature was less affected due to the lockdown. The temperature varied between 14-31°C and 14-30°C during the study period 2019 and 2020 respectively (Figure 5). Reduction in temperature was observed to be 0-5 % with respect to 2019. The highest reduction (5 %) was observed in the month of March 21 to April 10, 2020, during the period of lockdown (Figure 6).

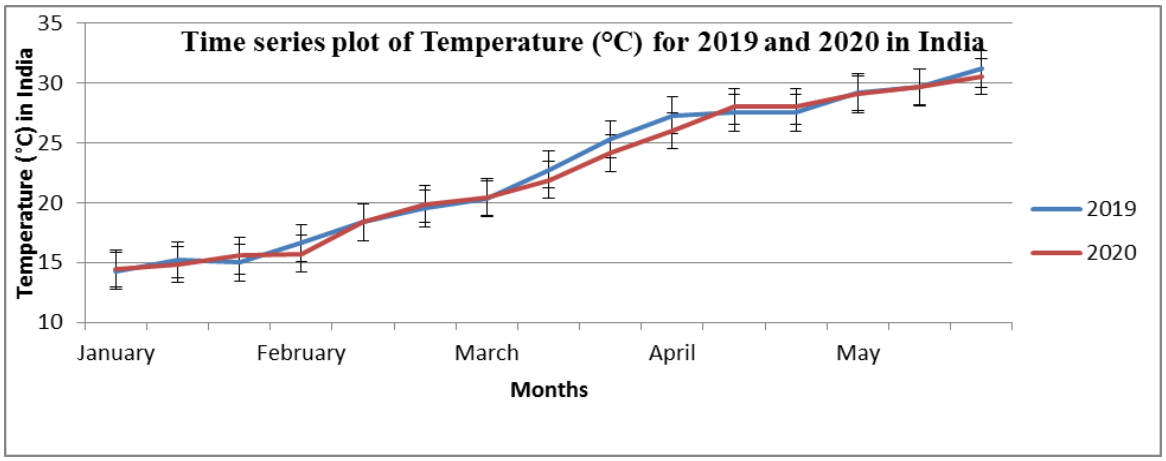

Fig 5. Time series plot of Temperature (°C) for 2019 and 2020 in India

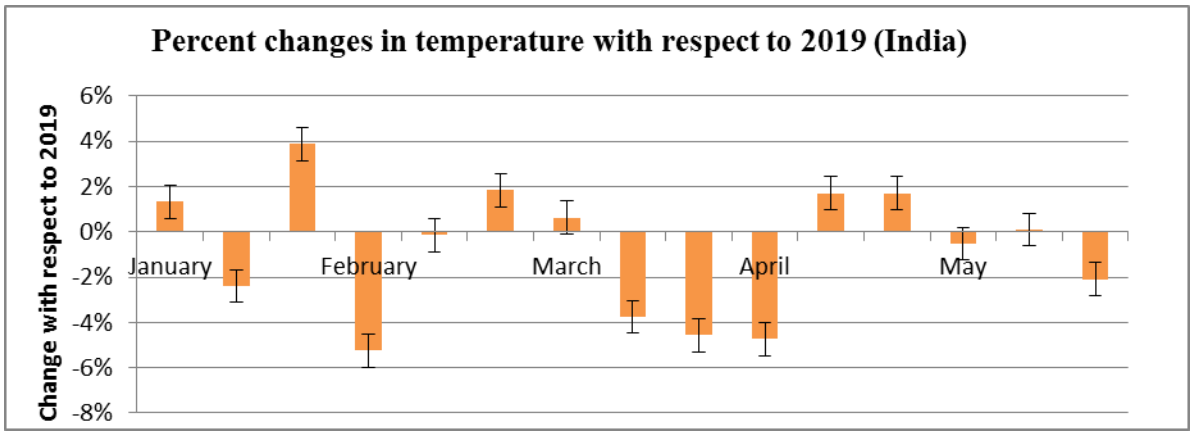

Fig 6. Total percentage change in Temperature (°C) of the year 2020 (Jan-May) with respect to 2019

3.4. NO_2 level in China

NO_2 concentration (mol/km²) in China, during (22 January to 8 April, 2020) and after (9 April to May 31, 2020) the partial lockdown represented in figure 7, illustrating that NO_2 concentration varied between 84-135 and 61-92 mol/km² during the entire study period of 2019 and 2020 respectively. A significant reduction was observed in NO_2 concentration ($P < 0.005$). Average reduction in the entire study period was 4-40 % with respect to 2019. The highest significant (40 %) reduction was found in the period of 21 January to 31 January, 2020 (Figure 8). Due to low industrial and vehicular activities, a significant reduction in NO_2 level was found in the partial lockdown period.

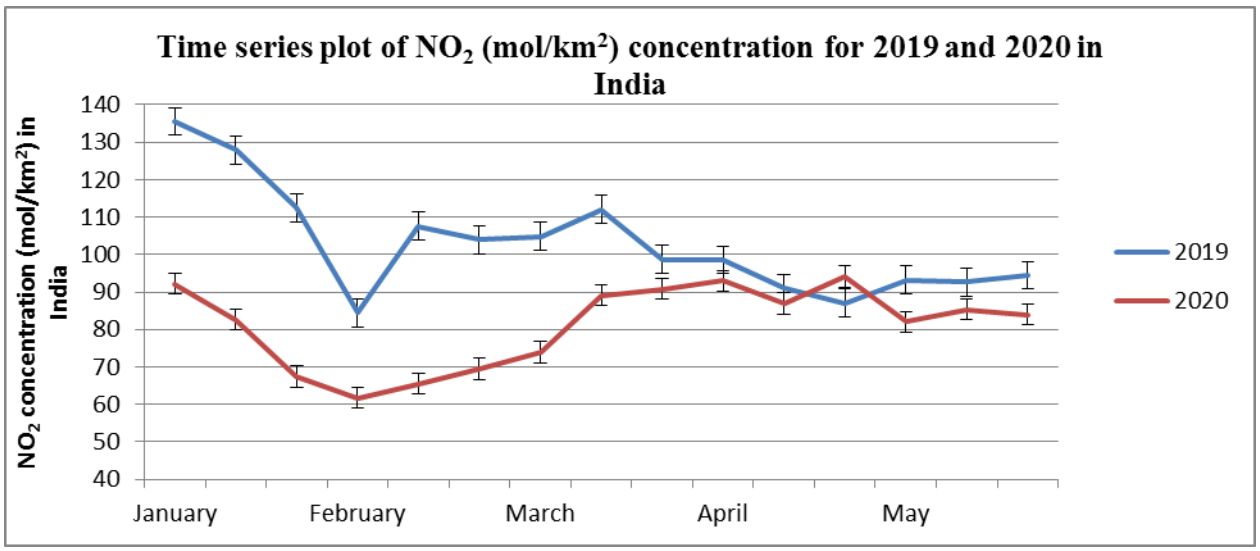

Fig 7. NO_2 concentration (mol/km²) for the year 2019 and 2020 in China

3.5. Ozone (stratospheric) level in China

In China, there was a significant increase in ozone level (mol/m2) in 2020 when compared to 2019. The study period was from 1st January to 31st May, and the ozone concentration ranged from 0.141-0.165 in 2019 and 0.143-0.162 in 2020 (Figure 9). During the study period, there was a 1-12 % percentage change in the ozone concentration. The highest percentage change (increase) in ozone concentration compared to 2019 was 11 % observed from 1st May to 10th May 2020 (Figure 10).

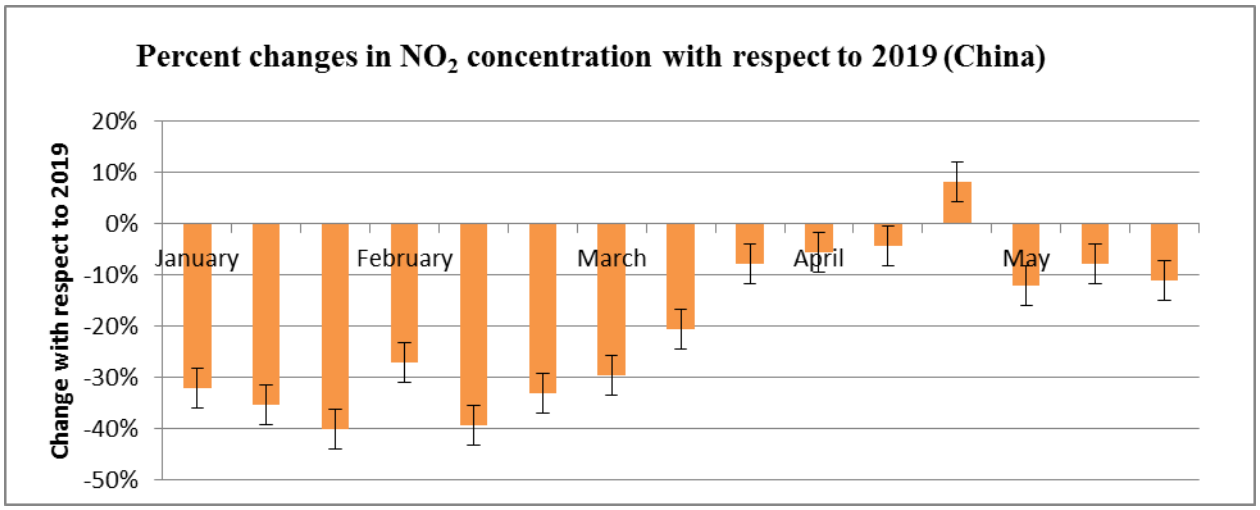

Fig 8. Total percentage change in NO_2 level of the year 2020 (Jan-May) with respect to 2019

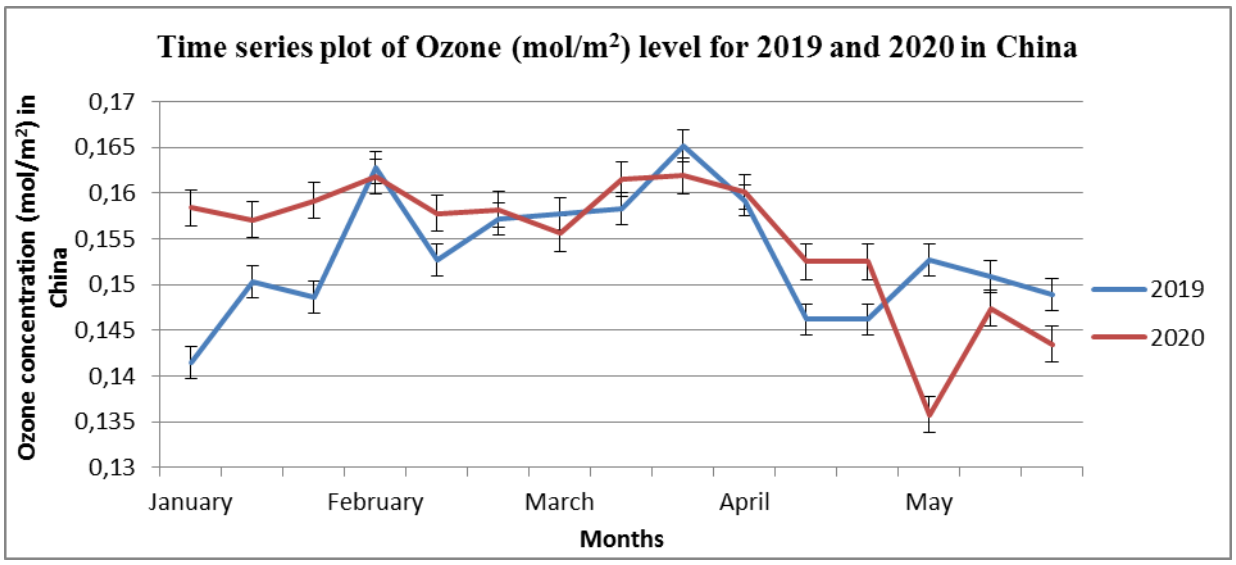

Fig 9. Time series plot of Ozone (mol/m²) level for 2019 and 2020 in India

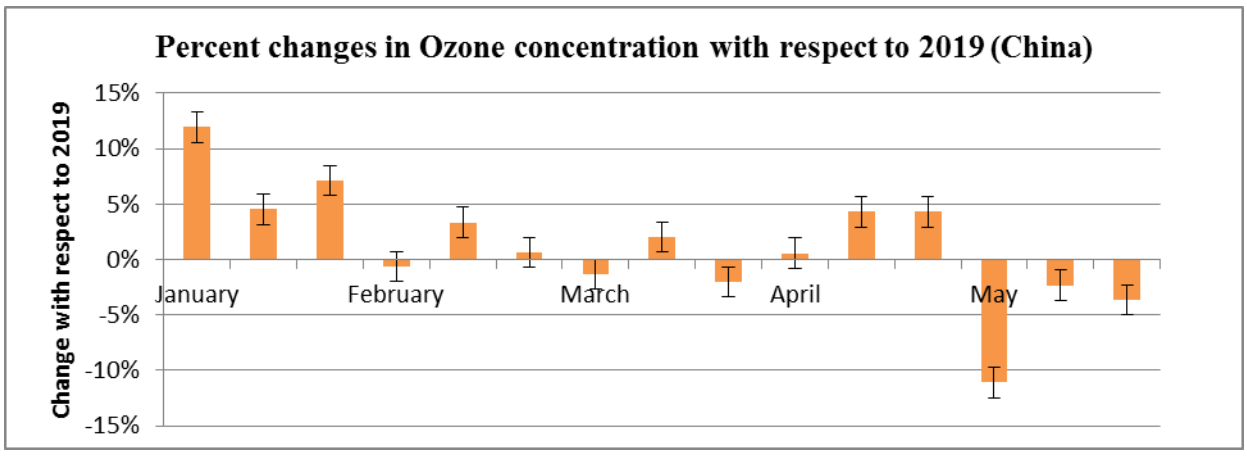

Fig 10. Total percentage change in Ozone level of the year 2020 (Jan- May) with respect to 2019

3.6. Temperature in China

The temperature range between -9°C to 15°C was observed in both 2019 and 2020, as demonstrated in Figure 11. Reduction in temperature varied between 1-94 % in entire study period (1 January – 31 May). The highest significant reduction from 11 March to 21 March, 2020 was 94 % (Figure 12) during which only essential services were allowed due to partial lockdown. This corresponded to a partial lockdown period that allowed only essential services to operate.

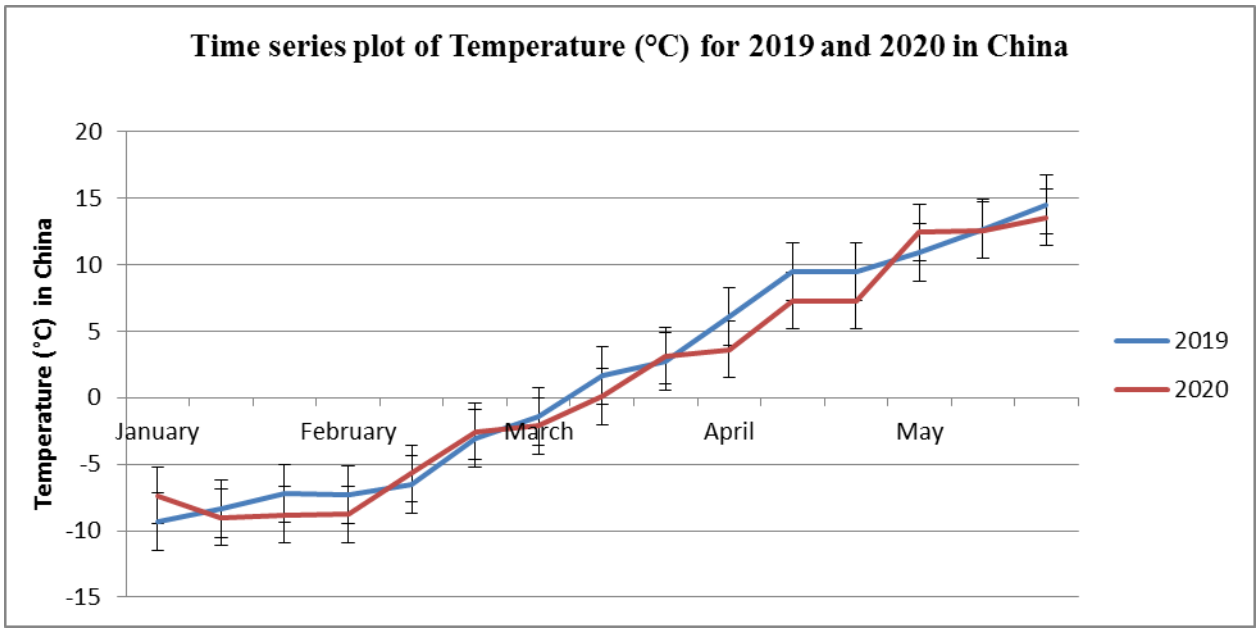

Fig 11. Time series plot of Temperature (°C) for 2019 and 2020 in India

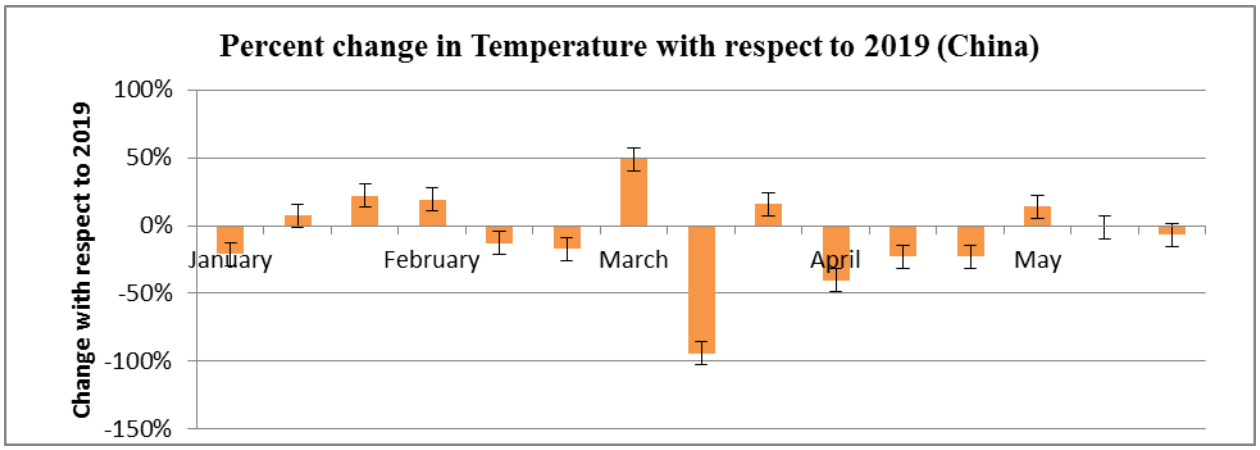

Fig 12. Total percentage change in Temperature (°C) of the year 2020 (Jan-May) with respect to 2019

3.7. NO_2 Tropospheric column from sentinel data

Figure 13 depicts sentinel images of NO_2 emission in India and China before, during, and after lockdown from 1 January to 31 May of both the year (2019 and 2020). According to this data, NO_2 emission has been reduced in April and May, 2020 as compared to 2019 in India. Similarly, in China NO_2 emission was reduced from January to May 2020 as compared to 2019.

That justifies that NO_2 emission was significantly reduced in the lockdown period in India and China during and after the lockdown period. The effect of lockdown is apparent on NO_2 emission on both the countries due to restrictions on industries and transport that led to less NO_2 emission.

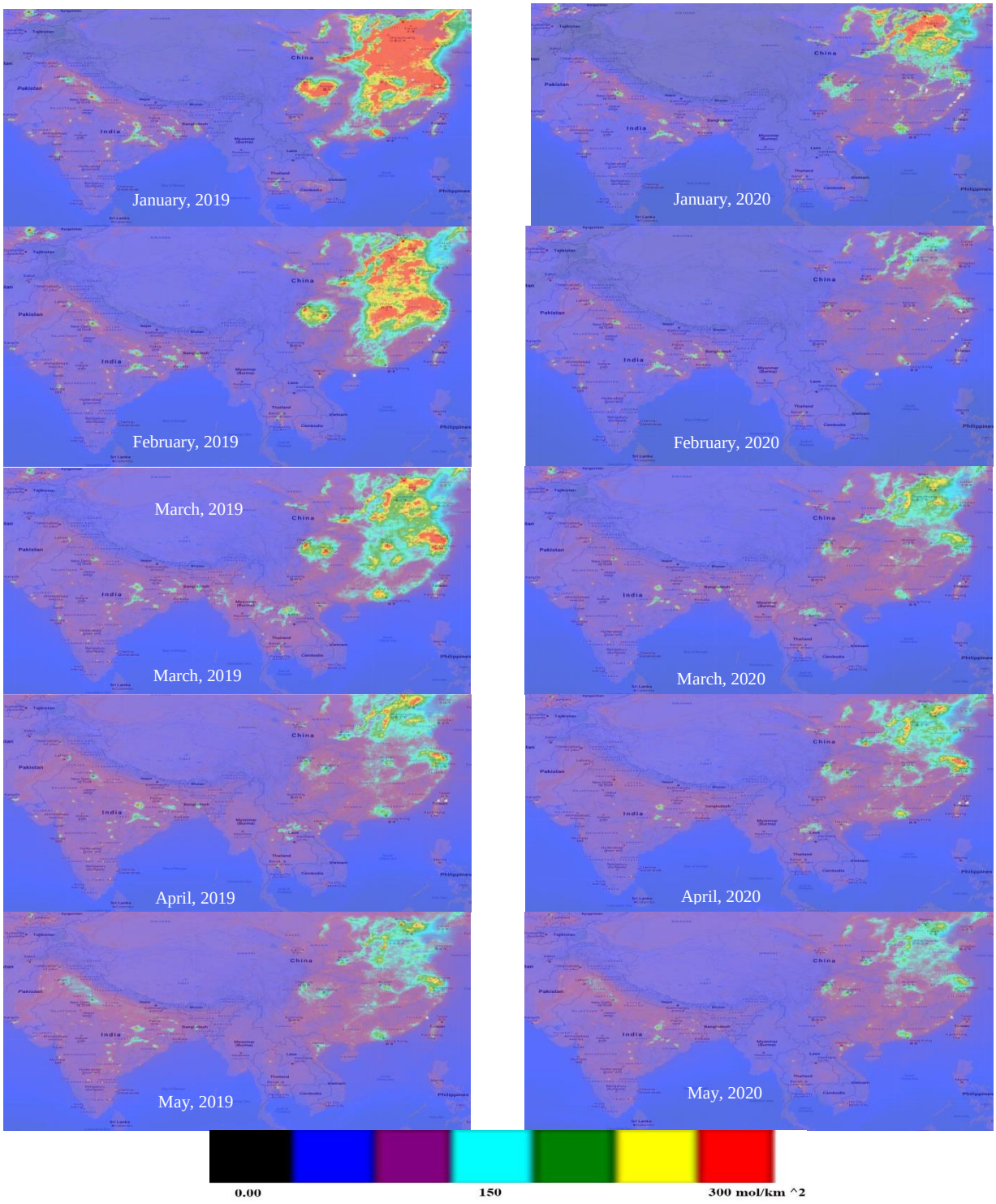

Fig. 13. NO_2 emissions in India and China before, during, and after the COVID-19 lockdown, based on data derived from Sentinel data

3.8. Stratospheric ozone column from sentinel data

Sentinel images of stratospheric ozone emission in India and China before, during, and after lockdown from 1 January to 31 May of both the year (2019 and 2020). According to the data of sentinel images, stratospheric ozone concentration in 2020 was higher than 2019 in both the countries from January to May (Figure 14). The effect of lockdown is apparent on Ozone concentration on both the countries due to restrictions on industries and transport that led to increase in stratospheric ozone concentration.

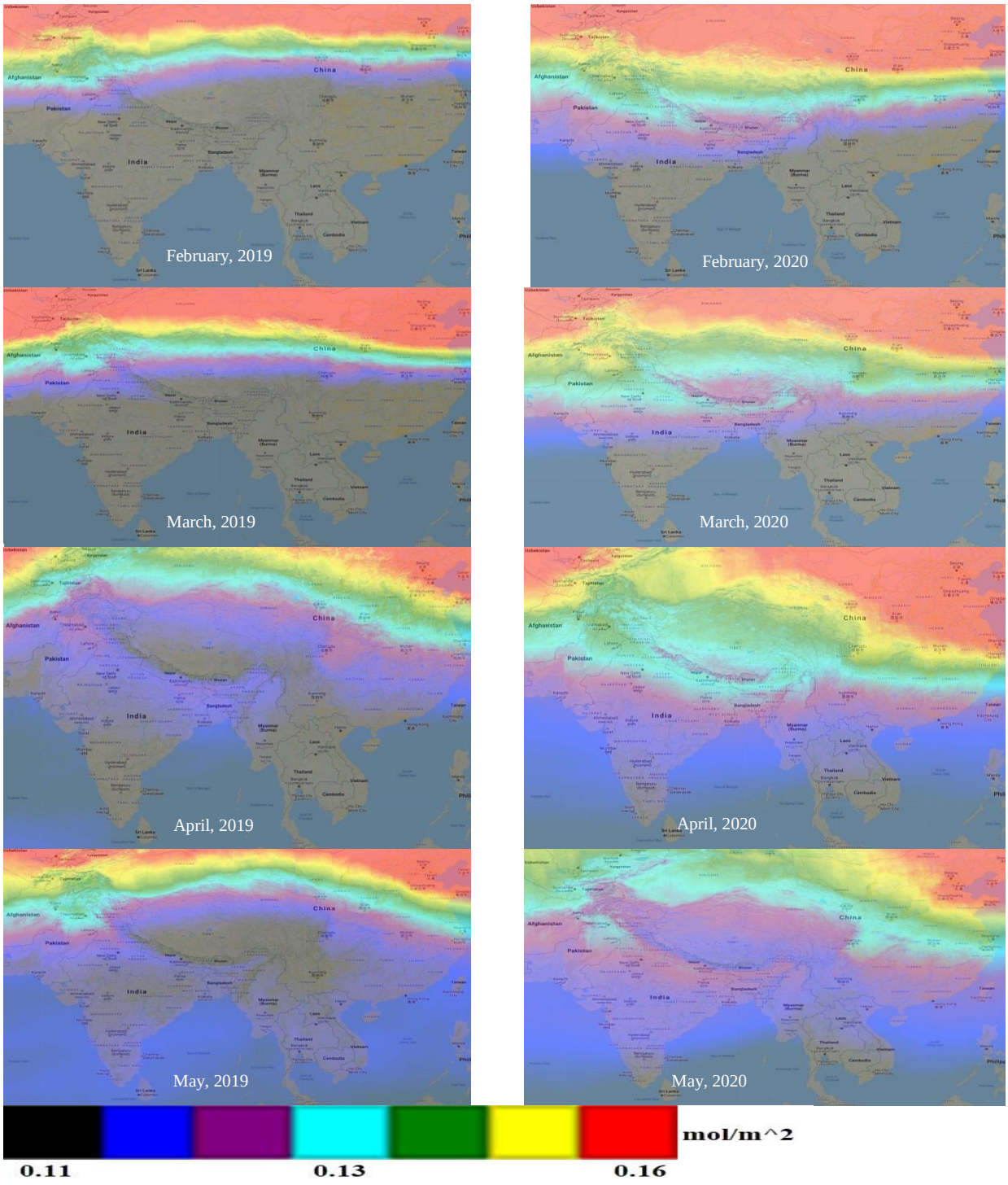

Fig 14. Stratospheric ozone concentration in India and China before, during, and after the COVID-19 lockdown, based on data derived from Sentinel data.

4. Conclusion

The findings of this study suggest that the COVID-19 lockdown had a significant impact on anthropogenic activities such as transportation and industrial activities, resulting in reduced NO2 emissions and an increase in stratospheric ozone concentration, as well as a decrease in global temperature rise. Comparing NO_2 emissions from 2020 to 2019, India and China saw significant reductions, with India's total reduction being 94 % from January to May, and China's total reduction being 298 % in the same period. Stratospheric ozone concentration increased significantly in both India and China, by 118 % and 18 %, respectively, and this also affected the temperature in both countries. The total temperature reduction in the same period was 12 % and

112% in India and China, respectively. The COVID-19 lockdown significantly impacted NO_2 emissions, ozone concentration, and temperature due to restrictions on transportation and decreased fuel combustion. While economic and social concerns were associated with the lockdown, the improvement in air quality can be seen as a positive consequence of COVID-19.

References

BBC, 2020 – Lockdowns rise as China tries to control virus. *United Kingdom: BBC.* 23 January 2020. Archived from the original on 23 January 2020. (date of access: 23.01.2020).

Bechle et al., 2013 – *Bechle, M.J., Millet, D.B., Marshall, J.D.* (2013). Remote sensing of exposure to NO2: satellite versus ground-based measurement in a large urban area. *Atmos. Environ.* 69: 345-353.

Bherwani et al., 2020 – *Bherwani, H., Gupta, A., Anjum, S., Anshul, A., Kumar, R.* (2020). Exploring dependence of COVID-19 on environmental factors and spread prediction in India. *Res. Square.* DOI: https://doi.org/10.21203/rs.3.rs-25644/v1

Chen et al., 2007 – *Chen, T.M., Kuschner, W.G., Gokhale, J., Shofer, S.* (2007). Outdoor air pollution: nitrogen dioxide, sulfur dioxide, and carbon monoxide health effects. *Am J Med Sci.* 333(4): 249-256.

Dentener et al., 2020 – *Dentener, F., Emberson, L., Galmarini, S., Capelli, G., Irimescu, A., Mihailescu, D., Van Dingenen, R., van den Berg, M.* (2020). Lower air pollution during COVID-19 lockdown: improving models and methods estimating ozone impacts on crops. *Phil. Trans. R. Soc. A.*

Eskes et al., 2019 – *Eskes, H., van Geffen, J., Boersma, F., Eichmann, K.-U., Apituley, A., Pedergnana, M., Sneep, M., Pepijn, J., Loyola, D.* (2019). Sentinel-5 precursor/TROPOMI Level 2 Product User Manual Nitrogendioxide document number: S5P-KNMI-L2-0021-MA.

Gautam, 2020 – *Gautam, S.* (2020). COVID-19: air pollution remains low as people stay at home. *Air Qual. Atmos. Health.* DOI: https://doi.org/10.1007/s1186 9-020-00842-6

Gautam, Hens, 2020a – *Gautam, S., Hens, L.* (2020a). SARS-CoV-2 pandemic in India: what might we expect? *Environ. Dev. Sustain.* 22: 3867-3.

Gautam, Trivedi, 2020 – *Gautam, S., Trivedi, U.K.* (2020). Global implication of bioaerosol in pandemic. *Environ. Dev. Sustain.* 22: 3861-3865.

Kumar et al., 2021 – *Kumar, D., Singh, A. K., Kumar, V., Poyoja, R., Ghosh, A., Singh, B.* (2021). COVID-19 driven changes in the air quality; a study of major cities in the Indian state of Uttar Pradesh. *Envir. Poll.* 274: 116512. DOI: https://doi.org/10.1016/j.envpol.2021.116512

Muhammad et al., 2020 – *Muhammad, S., Long, X., Salman, M.* (2020). COVID-19 pandemic and environmental pollution: A blessing in disguise? *Science of The Total Environment.* 728: 138820.

Nakada, Urban, 2020 – *Nakada, L., Urban, R.C.* (2020). COVID-19 pandemic: impacts on the air quality during the partial lockdown in São Paulo state, Brazil. *Sci. Total Environ.* 730: 5. DOI: https://doi.org/10.1016/j.scitotenv.2020.139087139087

Platt, Stutz, 2008 – *Platt, U., Stutz, J.* (2008). Introduction, in: Differential Optical Absorption Spectroscopy. Springer Berlin Heidelberg, pp. 1-4. DOI: https://doi.org/10.1007/978-3-540-75776-4_1

Regan et al., 2020 – *Regan, H., Mitra, E., Gupta, S.* (2020)."India places millions under lockdown to fight coronavirus. *CNN.*

Rodriguez-Morales et al., 2020 – *Rodriguez-Morales, A.J., Bonilla-Aldana, D.K., Tiwari, R., Sah, R., Rabaan, A.A., Dhama, K.* (2020). COVID-19, an emerging coronavirus infection: current scenario and recent developments – an overview. *J. Pure Appl. Microbiol.* 9.

Saha et al., 2014 – *Saha, S., Moorthi, S., Wu, X., Wang, J., Nadiga, S., Tripp, P., Behringer, D., Hou, Y.T., Chuang, H.Y., Iredell, M., Ek, M., Meng, J., Yang, R., Mendez, M.P., Van Den Dool, H., Zhang, Q., Wang, W., Chen, M., Becker, E.* (2014). The NCEP climate forecast system version 2. *J. Clim.* 27: 2185-2208. DOI: https://doi.org/10.1175/JCLI-D-12-00823.1

Sharma et al., 2020 – *Sharma, S., Zhang, M., Gao, J., Zhang, H., Kota, S.* (2020). Effect of restricted emissions during COVID-19 on air quality in India. *Sci. Total Environ.* 728: 138878.

Sentinel 5 – Sentinel 5 precursor/TROPOMI KNMI and SRON level 2 Input Output Data Definition. [Electronic resource]. URL: https://sentinel.esa.int/documents/247904/3119978/ Sentinel -5P-Level-2-Input-Output-Data-Definition

van Geffen et al., 2015 – *van Geffen, J.H.G.M., Boersma, K.F., Van Roozendael, M., Hendrick, F., Mahieu, E., De Smedt, I., Sneep, M., Veefkind, J.P.* (2015). Improved spectral fitting of nitrogen dioxide from OMI in the 405–465 nm window. *Atmos. Meas. Tech.* 8: 1685-1699. DOI: https://doi.org/10.5194/amt-8-1685-2015

Tobías et al., 2020 – *Tobías, A., Carnerero, C., Reche, C., Massagué, J., Via, M., Minguillón, M.C., Alastuey, A., Querol, X.* (2020). Changes in air quality during the lockdown in Barcelona (Spain) one month into the SARS-CoV-2 epidemic. *Sci. Total Environ.* 726: 138540.

van Geffen et al., 2019 – *van Geffen, J.H.G.M., Eskes, H.J., Boersma, K.F., Maasakkers, J.D., Veefkind, J.P.* (2019). TROPOMI ATBD of the total and tropospheric NO_2 data products. *Atmos. Meas. Tech.* 1.4.0: 1-76.

Veefkind et al., 2012 – *Veefkind, J.P., Aben, I., McMullan, K., Förster, H., de Vries, J., Otter, G., Claas, J., Eskes, H.J., de Haan, J.F., Kleipool, Q., van Weele, M., Hasekamp, O., Hoogeveen, R., Landgraf, J., Snel, R., Tol, P., Ingmann, P., Voors, R., Kruizinga, B., Vink, R., Visser, H., Levelt, P.F.* (2012). TROPOMI on the ESA Sentinel-5 Precursor: A GMES mission for global observations of the atmospheric composition for climate, air quality and ozone layer applications. *Remote Sens. Environ.* 120: 70-83. DOI: https://doi.org/10.1016/j.rse.2011.09.027

Wang et al., 2020 – *Wang, C., Horby, P.W., Hayden, F.G., Gao, G.F.* (2020). A novel coronavirus outbreak of global health concern. *Lancet*. 395(10223): 470-473.

Wang, Su, 2020 – *Wang, Q., Su, M.* (2020). Drivers of decoupling economic growth from carbon emission—an empirical analysis of 192 countries using decoupling model and decomposition method. *Environ. Impact Assess. Rev.* 106356: 81-92.

WHO, 2020a – WHO (World Health Organization). Coronavirus Disease 2019 (COVID-19) Situation Report-36, February 25, 2020. World Health Organization Geneva. [Electronic resource]. URL: https://www.who.int/docs/default-source/coronaviruse/situationreports/20200225-sitrep-36-covid-19.pdf?sfvrsn=2791b4e0_2

WHO, 2020b – WHO (World Health Organization). Coronavirus disease (covid-19) dashboard, global situation. 2020. [Electronic resource]. URL: http://who.covid19.int/

Published in the USA
Biogeosystem Technique
Issued since 2014.
E-ISSN: 2413-7316
2022. 9(2): 89-99

DOI: 10.13187/bgt.2022.2.89
https://bgt.cherkasgu.press

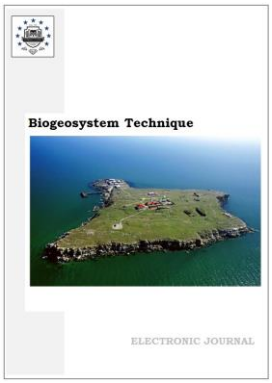

Assessing the Geo-Environmental Risks of Technogenic Pollution of Agricultural Soils

Astghik Sukiasyan [a, *], Arsen Simonyan [a], Samvel Kroyan [b], Alik Hovhannisyan [a], Vahram Vardanyan [c], Alla Okolelova [d], Armen Kirakosyan [a]

[a] National Polytechnic University of Armenia, Yerevan, Armenia
[b] National University of Architecture and Construction of Armenia, Yerevan, Armenia
[c] Yerevan State University, Yerevan, Armenia
[d] Volgograd State Technical University, Volgograd, Russian Federation

Paper Review Summary:
Received: 2022, June 14
Received in revised form: 2022, July 10
Acceptance: 2022, December 16

Abstract

Environmental problems are the result of the disturbance of the natural balance through a combination of processes in the environment and their irreversible consequences. The latter causes specific environmental problems. This is particularly true for countries with limited land, water and plant resources. Factors such as soil fertility and protection against adverse effects, inactivating and demobilising chemical pollutants that penetrate the soil, etc. must be managed to ensure a stable ecosystem. Climatic factors (ambient temperature, rainfall, wind rose, etc.) also contribute to wasteful human activities. All these factors lead to soil degradation and desertification in the territory of the Republic. There are different forms of these phenomena. The extent and irreversible consequences of heavy metal contamination of biota are well documented. However, all discussions are reduced to quantitative comparisons of heavy metal concentrations in the environment with accepted maximum permissible concentrations, without focusing on the nature of what is happening. In this article, approaches with consideration of geo-ecological coefficients for assessment of multi-component impact of anthropogenic pollution on arable soils of the Republic of Armenia are considered. The anthropogenic zone of the city of Hrazdan and the surrounding arable soils are considered as an example of the approach to the estimation of the degree of environmental pollution. It contributes to the differentiation of abiotic and anthropogenic factors of heavy metal pollution in environmental studies. It helps to differentiate between the abiotic and the anthropogenic sources of Heavy Metals in studying them. This approach makes it possible to set limits on the use of natural resources. It also contributes to the development of environmental protection measures aimed at the safety of the biota as a whole.

Keywords: heavy metals, pollution of soils, wind rose, Clark's coefficient, geoecological coefficients, monitoring.

* Corresponding author
E-mail addresses: sukiasyan.astghik@gmail.com (A. Sukiasyan)

1. Introduction

The combination of processes taking place in the environment and their irreversible consequences create environmental problems. They disrupt the ecological balance of the region (Third National Communication..., 2015). This leads to a number of environmental problems, especially in countries such as the Republic of Armenia, where the resources of land, water and plants are limited (Kroyan, 2019). Soil fertility and protection from adverse impacts, inactivating and demobilising penetrating chemical pollutants are important factors in ecosystem stability. All this is due to the complex structure and a variety of biochemical processes in the soil (Figure 1). It is known that in terms of origin, composition, structure and agronomic properties, the geochemical processes taking place under the conditions of vertical zoning of soils in Armenia have formed completely different genetic types of soils that alternate with each other from lowlands to high mountain peaks (Sukiasyan, 2018). The heterogeneous geological structure of the territory of the Republic of Armenia and the diverse nature of rock-forming excavations cause irreversible changes in the topography. As a result of these actions, there is contamination of all the components of the biota (Sukiasyan, Pirumyan, 2018).

On the other hand, the various manifestations of soil degradation (desertification, alkalinisation, etc.) and vegetation cover (Mkrtchyan, Petrosyan, 2014; https://unfccc.int) are caused by climatic changes together with wasteful human economic activities. In this regard, geo-ecological research, assessment and monitoring of the multifactorial effects of anthropogenic soil pollution of territories is necessary (Armenia. Climate..., 1999) due to the impact of uncontrollable anthropogenic factors on the ecosystem of the region.

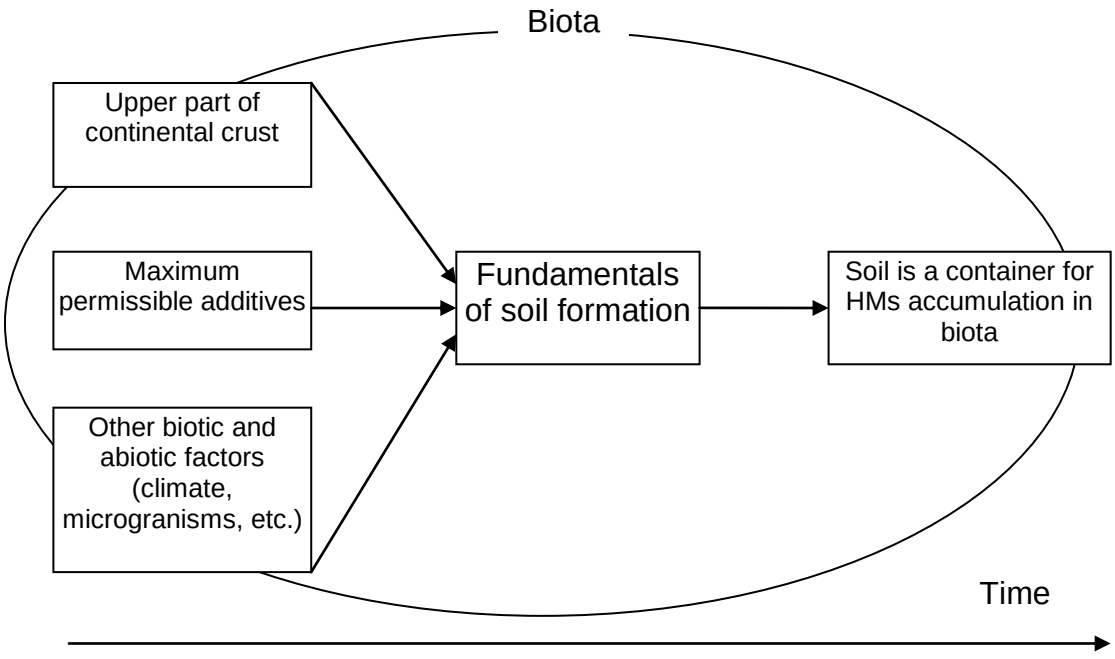

Fig. 1. Multi-component soil formation

One of the factors contributing to land degradation in Armenia is land contamination by mining industry, thermal power plants, chemical fertilizers for agriculture, transportation, etc. (Tepanosyan et al., 2018; Hunanyan, 2012; Danielyan, Khoetsyan, 2009). A combination of different monitoring approaches is necessary for the assessment of pollution of environmental components: biological condition of vegetation, soil water regime, pH response, nutrient inputs, organic carbon and other agrochemical indicators (Darzi-Naftchali, Ritzema, 2018; Shokri et al., 2022; Tchounwou et al., 2012; Ali et al., 2021). Environmental quality is effectively monitored by bioindication methods based on the determination of the ability of plants to absorb chemical elements from the growth soil (Parmar et al., 2016; Holt, Miller, 2010).

Among the dominant environmental pollutants are heavy metals (HMs), which are considered to be essential elements that are necessary as macro- and micro-nutrients for the biological activity of organisms (Pierzynski et al., 2000). Therefore, research on the mechanisms of HMs transport in the

food chain (soil-plant-human or soil-plant-animal-human) deserves special attention. They are highly dependent on the metal's chemical form, stimulating processes such as mineral deposition and dissolution, ion exchange, absorption and removal, biological immobilisation and mobilisation, as well as plant uptake and accumulation (Wuana, Okieimen, 2011).

However, many HMs are dangerous even at low concentrations. They can accumulate in the body and contribute to adverse effects (Yan et al., 2020). In addition, unlike organic pollutants, most HMs are not susceptible to microbiological or chemical degradation and can accumulate in the soil for long periods of time (Lasat, 2002). It is important to conduct comprehensive studies that will allow the study of the multi-component effects of anthropogenic pollution of natural soil zones in the Republic of Armenia. This will contribute to the ecological assessment of the quality and safety level of the environment, as well as to the development of monitoring methods. The Republic of Armenia is a mountainous country, with 77 per cent of its territory located at an average altitude of 1,850 metres above sea level. It is characterized by a complex combination of different relief structures, which leads not only to limited land and water use, but also to adverse engineering and geological conditions (high seismicity, abundance of geodynamic processes, etc.) of natural resources in general (Sagatelyan, 2004). The geographical position of the country and its complex mountainous terrain cause the diversity of natural conditions throughout the country. There are 14 types, 27 subtypes and many families, varieties and types of soils in Armenia, and the total number of soils is 228 (Resources ..., 2013). The most common types are mountain-meadow, mountain-brown forest, mountain-brown forest (the latter two types are grouped together with the forest humus-limestone types in the acrisol reference soil group); mountain-chernozem, mountain-chestnut (chestnut soils) and mountain-brown semi-desert (calcisols). The scattered variety of soils corresponds to the diversity of bioclimatic and lithological-geomorphological conditions of soil formation. The modern evolution of soils in the region is mainly determined by anthropogenic factors (Sagatelyan, 2004; Hunanyan, 2010), although they still exist in some places.

Agriculture is one of the developing sectors of the Armenian economy. The main source of water for irrigation of arable land is surface water and a small amount of groundwater (mainly in the Ararat Valley). Due to the presence of industrial, agricultural, cultural, municipal and other wastewater in these areas, the composition of water in rivers is subject to spatial and temporal changes. In addition, the use of polluted river water for irrigation leads to lower crop yields and deterioration of crop quality (Simonyan et al., 2018). In regions with a developed mining industry, HMs in irrigation water is in excess of permissible standards (Tutunjyan, Pirumyan, 2011). Potassium, iron, zinc and copper contents in river water fluctuate within the same limits in zones II and III (Figure 2).

The highest concentrations of iron, zinc and copper are found in zone I, which is largely due to the geochemical conditions of the area. The content of these metals decreases by 1.4 to 2.5 times (for zinc by 3.6 to 8.7 times) towards the south-east of the republic (zones II and III). On the contrary, from the north-western part of the country (zone I) to the central part (zone II) and the south-eastern part (zone III), the potassium content in Armenian river waters increases by 1.6 to 1.8 times. Selenium in river water increases uniformly and slowly, by a factor of 2 from zone I to zone II, and remains at low levels. In contrast to selenium, chromium in river waters increases significantly in Zone III (by a factor of 3), which is due to the development of mining and metallurgical industry in the Syunik region (Margaryan et al., 2014). The transport of HMs in soils is highly dependent on their chemical form. It stimulates the proliferation of processes such as mineral deposition and dissolution, ion exchange, adsorption and desorption, complex formation, biological immobilisation and mobilisation, uptake and accumulation by plants (Levy et al., 1992).

Soil is the ultimate site of deposition and accumulation of HMs. In contrast to organic pollutants, the majority of HMs are not subject to microbial or chemical degradation (Kirpichtchikova et al., 2006). Their total concentration in the soil persists for a long time (Adriano, 2001).

Fig. 2. Geographic zones of the studied rivers and their corresponding regions in Armenia: I zone is Northwestdirection with regions: Shirak, Lori, and Tavush; II zone is Midlle with regions: Aragatsotn, Kotayk, and Geharkunik; III zone is Southeast with regions Armavir, Ararat, Vayozh Dzor, and Syunik

At the same time, the presence of HMs in soil prevents the biodegradation of organic pollutants (Maslin, Maier, 2000). For an ecosystem, the contamination of soil by HMs poses potential risks through direct contact with contaminated soil via the food chain and through the use of contaminated groundwater (Mc Laughlin et al., 2000). The most important sources for the accumulation of HMs in the soil cover are summarised in Table 1. Among them, exploitation of metal mines, waste disposal in unprotected landfills and combustion of coal and petrochemical residues are more mobile and therefore more bioavailable than pedogenic or lithogenic (Korchagina, 2014).

Table 1. Anthropogenic sources of heavy metal accumulation in soils

Source of pollution	**Production type**	**Concentration coefficient (Кк)***	
		from 2 to 10	**more than 10**
Non-ferrous metallurgy	Production of non-ferrous metals directly from ores and concentrates	Pb, Zn, Cu, Ag	Sn, Bi, As, Cd, Sb, Hg, Se
	Secondary processing of non-ferrous metals	Pb, Zn, Sn, Cu	Hg
	Production of hard and refractory non-ferrous metals	W	Mo
	Titanium production	Ag, Zn, Pb, B, Cu	Ti, Mn, Mo, Sn, V
Iron and steel industry	Production of nonferrous metals	Co, Mo, Bi, W, Zn	Pb, Cd, Cr, Zn
	Iron ore Production	Pb, Ag, As	Zn, W, Co, W

Metal processing industry	Manufacture of superphosphate	Sr, Zn, F	Cu, Cr, As and rare-earth chemical elements
	Plastics production	-	Y, Ag
	Cement production	-	Hg, Sr, Zn
	Production of concrete products	-	-
Printing industry	Font foundries, printing houses	-	Pb, Zn, Sn
Solid domestic waste of large cities used as fertilizer	-	Pb, Cd, Sn, Cu, Ag, Sb, Zn	Hg
Sewage sludge	-	Pb, Cd, W, Ni, Sn, Cr, Cu, Zn	Hg, Ag
Wastewater for irrigation	-	Pb, Zn	Cu

* Note: K_k is the ratio of element content in the studied object to its background content.

2. Results and discussion

In intensive agriculture, large amounts of fertiliser are regularly applied to the soil to ensure the necessary crop growth. Approximately 10 % of the chemicals registered for use as pesticides, fungicides, insecticides and herbicides are based on compounds containing Cu, Hg, Mn, Pb or Zn (McMullen et al., 2009). They contain N, P and K as impurities as well as trace amounts of HMs (e.g. Cd and Pb), which significantly increase their content in the soil after long-term application (Song et al., 2013). In turn, application of animal manure, composts and compost mixes also accumulates trace elements As, Cd, Cr, Cu, Pb, Hg, Ni, Se, Mo, Zn, Tl, Sb, etc. in soil (Silva et al., 2012). One of the principles of sustainable waste management is the analysis of the potential impact of waste on the environment and the assessment of its potential impact. It is known that Pb, Ni, Cd, Cr, Cu and Zn are most commonly found in particulate matter of biological origin. When they enter the soil, they lead to leaching and contamination of groundwater (Li et al., 2014). Contaminants are therefore classified according to their hazardous environmental effects (Salt et al., 1998). However, regardless of the source of HMs (biotic or anthropogenic), any changes in environmental concentrations have global consequences. By their very nature, HMs contaminate all components of the biosphere (Król, 2011).

Fugitive emissions are often distributed over much smaller areas and close to the soil surface. The type and concentration of HMs thus released is dependent on the specific conditions that cause their deposition on the soil surface (Crommentuijn et al., 1997). Further development of the rock weathering scenario is accompanied by the penetration of simple and complex HMs ions into clay minerals. This is associated with subsequent binding to soil organic matter (Dobrovolsky, 1983). Changes in the concentration of HMs in air, surface water and groundwater result from this distribution.

The upper (sedimentary and granitic-metallic) layer of the continental crust is the main reservoir for the accumulation of HMs. The experimental sites of our experiments have a complex chemical composition of the geological structure of rocks, which is characteristic of the coastal

areas of large rivers. Therefore, it is reasonable to consider Clark's coefficient (K_k) of chemical elements as a reference (Vodiansky, 2012; Sukiasyan, 2018). Differences in the prevalence of geochemical anomalies of the studied chemical elements were revealed according to the calculated results of Kk in the surface soil horizon of the experimental sites (Table 2).

Table 2. The values of Clark`s coefficient of soil samples from different soil-climate regions of the Republic of Armenia

Chemical element	Hushakert	Odzun	Shnokh	Teghut	Hrazdan	Gavar	Martuni	Condition control
Ba	0.18	0. 42	1. 21	0. 49	0.85	0.89	1.36	0.98
Sr	0.69	0. 58	0. 55	0. 49	1.66	2.03	2.84	1.29
Rb	1.20	20. 8	2. 29	2. 61	4.42	3.43	8.58	4.08
As	3.14	1. 96	8. 38	1. 70	8.02	4.83	7.19	3.02
Pb	0.80	1. 04	4. 34	0. 68	8.47	5.52	5.66	2.14
Zn	1.32	0. 87	3. 39	0. 72	1.30	1.18	2.28	2.35
Cu	1.64	2. 66	16. 14	1. 24	2.09	2.12	3.68	2.23
Ni	1.11	0. 88	1. 27	1. 19	1.31	1.65	2.85	1.67
Co	14. 24	12. 75	14. 58	7. 08	4.94	8.62	7.61	9.48
Fe	1. 08	0. 54	0. 66	0. 52	0.72	0.95	1.55	0.90
Mn	1. 30	0. 55	0. 87	0. 59	1.09	1.07	1.92	1.16
Cr	4. 02	1. 07	0. 76	0. 78	1.13	1.28	2.94	2.07
V	1. 93	1. 01	0. 96	0. 91	1.05	1.11	1.93	1.12
Ti	0. 78	0. 72	0. 78	0. 81	0.95	1.12	2.05	1.21
Ca	1. 23	1. 20	0. 66	0. 93	0.51	0.61	1.87	1.15
K	0. 29	0. 51	0. 55	0. 62	0.71	0.59	1.23	0.61
S	trace	0. 41	0. 53	0. 312	1.36	0.98	1.42	0.32

*Note: Marked chemical elements have no Clark's value to calculate the coefficient (K_k), and if $K_k > 10$, the content of concentrations of chemical elements in soil samples is high; if $1.6 < K_k < 10$, then the content of concentrations of chemical elements in soil samples is average; if $1.0 < K_k < 1.5$, then the concentration of the chemical element in soil samples is poor (Grigoryev, 2009).

The distribution of chemical elements in the environment is influenced by many factors: the distance from the source of pollution and its power; the quantity and composition of gas and dust emissions reaching the soil; the transformation of the element and the state of its compounds; the properties and composition of the soil, the dynamics of soil processes, etc. With the most modern technological production schemes, a significant amount of highly toxic compounds can be released into the environment, polluting the atmospheric air, the water and the soil of the regions in equal measure. The danger of elevated levels of HMs in an ecosystem is that most chemical elements are highly biologically active (Singh et al., 2011). HMs are the second most dangerous substances (after pesticides), but far ahead of carbon dioxide and sulphur dioxide, which may become more dangerous than nuclear power plant waste and solid waste in the future (Santa-Cruz J et al., 2021; Aschmann, 2019). As a result of their dispersion through air currents, they reach the land cover and the water surface, while as a result of migration they accumulate and enter the trophic chain in various components of the biota (Mishra et al., 2019; Etim et al., 2021; Dovletyarova et al., 2022; Sukiasyan et al., 2020). Consider the situation of arable land contamination using the example of the industrial zone surrounding the city of Hrazdan, which is one of the most important industrial and energy centres in the Republic of Armenia. The Hrazdan Thermal Power Station (HTPS) and the Hrazdan Cement Plant (HCP) are located here. Other important enterprises are also located here. In this case, it is mainly the quality, grade and type of natural material that determines the toxicity of the flue and exhaust gases emitted into the air. In addition, being close to a gas turbine power station only exacerbates the uncontrolled pollution that can be caused by heat engines and plants burning hydrocarbon fuels. This is the reason why pollution in Hrazdan constantly exceeds the maximum permissible concentrations by almost 8 times (Resources..., 2013). The degree of danger of pollutant emissions from thermal power plants may be due to the low quality of the raw materials used, which implies the presence of a large number of accompanying impurities. Airborne pollutants enter the soil where they accumulate as a result of

migration and enter various biota (Kumar et al., 2008; Sukiasyan, Kirakosyan, 2020). Such a unique natural reservoir can "reflect" not only in situ pollution processes, but also those that occurred long ago (Levshakov, 2011).

A qualitative analysis of the soils in terms of the degree of contamination is crucial to solving the problem of the ecological state of the region (Blaser et al., 2000). In our studies, the soil cover is mainly represented by chestnut soils and chernozems. These soils are characterised by the loss of the upper fertile layer during industrial pollution (Kroyan et al., 2021). Special consideration was given to the peculiarities of the wind direction in the area. In cement production, the pollutants that spread in the atmosphere and are gradually deposited on the soil contain different HMs (Arfala et al., 2018). It has been shown that the largest percentage decrease in HMs content with distance from the source has been recorded for Pb, slightly less for Zn and Cu, averaging 52 % (Rühling, Tyler, 2001).

In a series of experiments, the influence of anthropogenic pollution in the vicinity of industrial enterprises in Armenia was determined in samples of arable soils taken at a distance of 0.5, 1.5, 2.5, 5, 10, 15 and 25 km from the source of pollution. In particular, the peculiarities of the direction of the wind rose in the area were taken into account. According to the results, the highest values of the content of the studied HMs in the anthropogenic HCP zone were recorded in the range of 0.5-2.5 km as the following comparative series Zn> Pb> Cu. The average concentration of Zn and Pb decreased by 78% and Cu by 53% at a distance of 25 km from the plant. The order of comparison for the pollutants under investigation was Zn > Cu > Pb > Co > Mo (Sukiasyan et al, 2021). Based on the values of concentrations of some chemical elements, coefficients were calculated (the risk of soil contamination (K_o) and the total pollution index (Z_c)). These coefficients made it possible to assess the degree of anthropogenic load and the level of soil pollution (Sukiasyan, 2018; Kasimov, Vlasov, 2015; Müller, 1981). Thus, in the vicinity of the HCP, a low level of pollution was indicated by the values of Z_c within 5 km. Changes in the coefficient were about 90 % at a further distance of 25 km from the source of contamination. The highest risk of soil contamination in the vicinity of the HCP was lead (K_o = 2.9). This risk was maintained up to a distance of 5 km from the source, after which there was a sharp decrease. A similar situation was observed for zinc (K_o = 2.3). Pollution by copper compounds was consistently high (Sukiasyan et al, 2021). These experiments were continued to determine the effect of the wind rose at a distance of up to 1 km using the example of the Hrazdan industrial zone. Concentrations of As and Pb decreased on average by 27 % with increasing distance from the industrial zone in the city of Hrazdan (Table 3). In quantitative terms, the concentration of lead was three times higher than that of arsenic along the sampling line.

Table 3. The value of Clark`s coefficient (K_k), the coefficient of soil contamination hazard level (K_o) and the total contamination index (Z_c) near the Hrazdan industrial zone

Distance from the source of pollution (Hrazdan industrial zone), km	As		Pb		Zn		Cu		Ni		Co		Z_c
	K_k	K_o	K_k	K_o	K_k	K_o	K_k	K_o	K_k	K_o	K_k	K_o	
1.0	7.27	4.07	7.44	3.95	1.39	1.16	1.97	1.69	1.43	10.66	1.79	3.36	16.29
0.8	8.11	4.54	9.92	5.27	1.07	0.89	1.54	1.32	1.45	10.81	0	-	17.09
0.6	9.02	5.05	9.73	5.17	1.19	0.98	1.86	1.59	1.15	8.61	0	-	17.95
0.4	9.48	5.31	9.76	5.19	1.23	1.02	1.70	1.45	1.40	10.46	0	-	18.58
0.2 (near industrial zone)	9.88	5.53	10.34	5.49	1.01	0.84	1.60	1.37	1.14	8.49	0	-	18.96

*Note: The value of K_o> 1 pollution level was high danger; ** the summary pollution level was classified as low with Z_c< 16 contamination is considered as non-dangerous; with 16 < Z_c <

32 contamination is moderately dangerous; with 32 < Z_c < 128 contamination is dangerous; with Z_c > 128 contamination is extremely dangerous (Müller, 1981).

Soil samples show an average 25.5 % increase in zinc and nickel and a 19% increase in copper concentrations away from the source of pollution. Cobalt is also of particular interest. Its traces were found in soil samples close to the source of pollution. This is why the value of Clark's coefficient is zero. Already along the sampling line, at a distance of one kilometre, its concentration in soil samples was 84.0 mg/kg, which made it possible to calculate K_k. Then, the calculation of some coefficients K_o and Z_c, taking into account Clark's coefficient for each of the HMs, allows to determine the possibility of its migration, taking into account the wind rose (see Table 3).

In a situation where the coefficient is K_o > 1, especially in the vicinity of the source of contamination, it can take on exorbitant values. According to the established criteria, the risk of contamination increases in direct proportion to the content of HMs in the studied samples, taking into account their maximum allowable concentration (Sukiasyan, 2018). A moderately hazardous level of contamination was found in the soil samples collected in the study areas at a distance of 0.2 km from the source of contamination. The value of the total pollution index (Z_c) decreased by 16 % with increasing distance from the enterprises. As we move away from the sources up to 1 km, there is a significant increase in the concentrations of other elements (Ni, Co, Cu and Zn). The processes of migration of HMs in anthropogenically polluted areas may be due to the dominance of the southwest direction of the wind rose in this region, and a comparative line is presented as a sequence: As < Ni < Co < Cu < Zn < Pb.

3. Conclusion

Information on the extent and irreversible consequences of HMs contamination of biota is abundant. However, without going into the nature of the anomaly, all discussions about the created situation are ultimately reduced to a comparison of changes in the concentration of HMs in the environment with the accepted maximum permissible concentrations. The proposed analysis of the current situation on the example of the assessment of the technogenic zone of the city of Hrazdan brings to the fore in geo-ecological studies the concept of differentiation between abiotic and anthropogenic pollution of HMs and possible ways of their migration on the basis of the developed approach to the assessment of pollution. The choice of this approach makes it possible to apply clear limits to the use of natural resources and, to some extent, contributes to the development of conservation measures aimed at preserving the biota as a whole.

4. Acknowledgements

The work was supported by the Science Committee of MESCS RA, in the frames of the research project № 21T-2H216 and № 15T-2H409. The authors express thanks to Mr. M. Aslikyan and Mr. A. Galstyan from the RA NAS “National Bureau of Expertises” SNPO for their support in measuring the concentration of chemical elements using the “Termo Scientific™ Niton™ XRF Portable Analyzer” X-ray fluorescence analyzer.

References

Adriano, 2001 – *Adriano, D.C.* (2001). Trace Elements in Terrestrial Environments: Biogeochemistry, Bioavailability and Risks of Metals, Springer, New York, USA, 2nd edition. 867 p. DOI: http://dx.doi.org/10.1007/978-0-387-21510-5

Ali et al., 2021 – *Ali, M. M., Hossain, D., Al-Imran, A., Khan, M. S., Begum, M., Osman, M. H.* (2021). Environmental Pollution with Heavy Metals: A Public Health Concern. In M. K. Nazal, & H. Zhao (Eds.), Heavy Metals – Their Environmental Impacts and Mitigation. IntechOpen. DOI: https://doi.org/10.5772/intechopen.96805

Arfala et al., 2018 – *Arfala, Y., Douch, J., Assabbane, A., Kaaouachi, Kh., Tianc, H., Hamdani, M.* (2018). Assessment of heavy metals released into the air from the cement kilns co-burning waste: Case of Oujda cement manufacturing (Northeast Morocco). *Sustainable Environment Research*. 28(6): 363-373. DOI: https://doi.org/10.1016/j.serj.2018.07.005

Armenia. Climate..., 1999 – Armenia. Climate. Change Issues / Collection of Articles, Editor: A. Gabrielyan. Yerevan, 1999. 373 p. Fourth National Communication on Climate Change –UNFCCC. [Electronic resource]. URL: https://unfccc.int/sites/default/files/resource/NC4_Armenia_pdf

Artemyev, 1990 – *Artemyev, V.G.* (1990). Chemical substances in the environment. M.

Aschmann, 2019 – *Aschmann, M.* (2019). Addressing air pollution and beyond in Ulaanbaatar: The role of sustainable mobility. *Geography, Environment, Sustainability*. 12(3): 213-223. DOI: https://doi.org/10.24057/2071-9388-2019-30

Crommentuijn et al., 1997 – *Crommentuijn, T., Polder, M.D., Van de Plassche, E.J.* (1997). Maximum permissible concentrations and negligible concentrations for metals, considering background concentrations. RIVM Report 601501 001. National Institute of Public Health and the Environment, Bilthoven, The Netherlands, 260 p.

Danielyan, Khoetsyan, 2009 – *Danielyan, K., Khoetsyan, A.* (2009). "GEO-cities" process in Armenia: experience gained, identified problems, possible prospects 2009. *Caucasian Geographical Journal*. 10: 153-157.

Darzi-Naftchali, Ritzema, 2018 – *Darzi-Naftchali, A., Ritzema, H.* (2018). Integrating Irrigation and Drainage Management to Sustain Agriculture in Northern Iran. *Sustainability*. 10(6):1775. DOI: https://doi.org/10.3390/su10061775

Dobrovolsky, 1983 – *Dobrovolsky, V.V.* (1983). Geography of trace elements. Global dispersion. oscow: Mysl. 271 p.

Dovletyarova et al., 2022 – *Dovletyarova, E., Fareeva, O., Brykova, R., Karpukhin, M., Smorkalov, I., Brykov, V., Gabechaya, V., Vidal, K., Komárek, M., Neaman, A.* (2022). Challenges in Reducing Phytotoxicity of Metals in Soils Affected by Non-Ferrous Smelter Operations. *Geography, Environment, Sustainability*. 15(1): 112-121. DOI: https://doi.org/10.24057/2071-9388-2021-141.

Etim et al., 2021 – *Etim, M-A., Babaremu, K., Lazarus, J., Omole, D.* (2021). Health Risk and Environmental Assessment of Cement Production in Nigeria. *Atmosphere*. 12(9): 1111. DOI: https://doi.org/10.3390/atmos12091111

Grigoryev, 2001 – *Grigoryev, N.A.* (2001). Distribution of chemical elements in the upper part of the continental crust. Yekaterinburg: UrO RAS, 2009, 382 p.

Holt, Miller, 2010 – *Holt, E.A., Miller, S.W.* (2010). Bioindicators: Using Organisms to Measure Environmental Impacts. *Nature Education Knowledge*. 3(10): 8.

Hunanyan, 2010 – *Hunanyan, S.A.* (2010). Agromonitoring of ecosystems in technogenic zones of the Republic of Armenia and development of measures for rehabilitation of soil fertility. Yerevan. 40 p.

Hunanyan, 2012 – *Hunanyan, S.A.* (2012). Influence of technogenic emissions on agrochemical indicators of soils in the vicinity of the Vanadzor chemical plant of the Republic of Armenia. *News of Agrarian Science*. 10(3): 41-44.

Kasimov, Vlasov, 2015 – *Kasimov, N., Vlasov, D.* (2015). Klarki khimicheskikh elementov kak etalony sravneniya v ekogeokhimii [Clarkes of chemical elements as reference standards in ecogeochemistry]. *Vestnik Moskovskogo universiteta. Seriya 5. Geografiya*. 2: 7-17. [in Russian]

Kirpichtchikova et al., 2006 – *Kirpichtchikova, T.A., Manceau, A., Spadini, L., Panfili, F., Marcus, M.A., Jacquet, T.* (2006). Speciation and solubility of heavy metals in contaminated soil using X-ray microfluorescence, EXAFS spectroscopy, chemical extraction, and thermodynamic modelling. *Geochimica et Cosmochimica Acta*. 70(9): 2163-2190.

Korchagina, 2014 – *Korchagina, K.V.* (2014). Assessment of urban soil pollution by heavy metals taking into account the profile distribution of their volumetric concentrations. Moscow. 145 p.

Król, 2011 – *Król, A.* (2011). Problems of assessment of heavy metals leaching from construction materials to the environment. *Architecture Civil Engineering Environment*. 4(3): 71-76.

Kroyan et al., 2021 – *Kroyan, S., Sukiasyan, A., Jabbarov, Z.* (2021). Study of some changes in water-physical properties of *Kastanozems*. *Land of Uzbekistan*. 4: 8-12.

Kroyan, 2019 – *Kroyan, S.* (2019). State of the main soil types in the Republic of Armenia under the conditions of climate change. *Soil Science and Agrochemistry*. 1: 5-18.

Kumar et al., 2008 – *Kumar, S., Singh, N., Kumar, V., Sunisha, B., Preeti, Sh., Deepali, S., Nath, Sh.R.* (2008). Impact of dust emission on plant vegetation in the vicinity of cement plant. *Environ EngManag J*. 7: 31-35. doi: 10.1145/1346256.1346261.

Lasat, 2021 – *Lasat, M.M.* (2021). Phytoextraction of toxic metals: a review of biological mechanisms. *J. Environ. Qual*. 31(1): 109-120.

Levshakov, 2011 – *Levshakov, L.* (2011). Rationing of the content of heavy metals in the soil. *Bulletin of the Kursk State Agricultural Academy*. 3: 51-53.

Levy et al., 1992 – *Levy, D.B., Barbarick, K.A., Siemer, E.G., Sommers, L.E.* (1992). Distribution and partitioning of trace metals in contaminated soils near Leadville, Colorado. *Journal of Environmental Quality*. 21(2): 185-195.

Li et al., 2014 – *Li, Y., Yang, R., Zhang, A., Wang, S.* (2014). The distribution of dissolved lead in the coastal waters of the East China Sea. *Marine Pollution Bulletin*. 85: 700-709.

Margaryan et al., 2014 – *Margaryan, L.A., Tokmajyan, L.V., Mkrtchyan, S.M.* (2014). Spatial-temporal trends of changes of the ra river water mineralization Bulletin of NPUA. *Series Hydrology and Hydraulic Engineering*. 2: 41-45.

Maslin, Maier, 2000 – *Maslin, P., Maier, R.M.* (2001). Rhamnolipid-enhanced mineralization of phenanthrene in organic-metal co-contaminated soils. *Bioremediation Journal*. 4(4): 295-308.

McLaughlin et al., 2000 – *McLaughlin, M.J., Hamon, R.E., McLaren, R.G., Speir, T.W., Rogers, S.L.* (2000). Review: a bioavailability-based rationale for controlling metal and metalloid contamination of agricultural land in Australia and New Zealand. *Australian Journal of Soil Research*. 38(6): 1037-1086.

McMullen et al., 2009 – *McMullen, M. D., Kresovich, S., Villeda, H. S., Bradbury, P., Li, H., Sun, Q., Flint-Garcia, S., Thornsberry, J., Acharya, C., Bottoms, C., Brown, P., Browne, C., Eller, M., Guill, K., Harjes, C., Kroon, D., Lepak, N., Mitchell, S. E., Peterson, B., Pressoir, G., Buckler, E.S.* (2009). Genetic properties of the maize nested association mapping population. *Science (New York, N.Y.)*. 325(5941): 737-740. DOI: https://doi.org/10.1126/science.1174320

Mishra et al., 2019 – *Mishra, S., Bharagava, R., More, N., Yadav, A., Zainith, S., Mani, S.* (2019). Heavy metal contamination: an alarming threat to environment and human health. In: Environmental biotechnology: For sustainable future. Springer: 103-125.

Mkrtchyan, Petrosyan, 2014 – *Mkrtchyan, A.L., Petrosyan, G.G.* (2014). Climate changes and soil degradation in Armenia. *Annals of Agrarian sciens, Tbilisi, Georgia*. 12: 42-46.

Müller, 1981 – *Müller, G.* (1981). Die Schwermetalbelastung der sedimente des Neckars und seiner Nebenflusse Eine Bestandsaufnahme. *Chemical Zeitung*. 105:157-164.

Parmar et al., 2016 – *Parmar, T.K., Rawtani, D., Agrawal, Y.K.* (2016). Bioindicators: the natural indicator of environmental pollute on. *Frontiers in Life Science*. 9 (2):110-118. DOI : https://doi.org/10.1080/21553769.2016.1162753

Pierzynski et al., 2000 – *Pierzynski, G.M., Sims, J.T., Vance, G.F.* (2000). Soils and Environmental Quality, CRC Press, London, UK, 2nd edition.

Resources..., 2013 – Resources of Mediterranean and Caucasus Countries /Ed.: Yigini Y., Panagos P., Montanarella L. Luxembourg: Publications Office of the EU, 2013, 243 p. DOI: 10.2788/91322.

Rühling, Tyler, 2001 – *Rühling, A., Tyler G.* (2001). Changes in atmospheric deposition rates of heavy metals in sweden a summary of Nationwide Swedish Surveys in 1968/70–1995. *Water, Air, & Soil Pollution: Focus*. 1: 311-323. DOI: 10.1023/A:1017584928458.

Sagatelyan, 2004 – *Sagatelyan, A.K.* (2004). Features of distribution of heavy metals on the territory of Armenia: Monograph. Yerevan: Publishing house of Center for Ecological and Oosphere Studies of NAS RA. 154 p.

Salt et al., 1998 – *Salt, D.E., Smith, R.D., Raskin, I.* (1998). Phytoremediation. *Annual Reviews in Plant Physiology & Plant Molecular Biolog*. 49: 643-668.

Santa-Cruz et al., 2021 – *Santa-Cruz, J., Peñaloza, P., Korneykova, M., Neaman, A.* (2021). Thresholds of metal and metalloid toxicity in field-collected anthropogenically contaminated soils: A Review. *Geography, Environment, Sustainability*. 14(2): 6-21. DOI: https://doi.org/ 10.24057/2071-9388-2021-023.

Shokri et al., 2022 – *Shokri, S., Abdoli, N., Sadighara, P., Mahvi, A.H., Esrafili, A, Gholami, M., Jannat, B., Yousefi, M.* (2022). Risk assessment of heavy metals consumption through onion on human health in Iran. *Food chemistry: X*. 14: 100283. DOI: https://doi.org/ 10.1016/j.fochx.2022.100283

Silva et al., 2012 – *Silva, N.D.G., Cholewa, E., Ryser, P.* (2012). Effects of combined drought and heavy metal stresses on xylem structure and hydraulic conductivity in red maple (*Acer rubrum* L.). *Journal of Experimental Botany*. 63: 5957-5966.

Simonyan et al., 2018 – *Simonyan, G.S., Simonyan, A.G., Pirumyan, G.P.* (2018). Analysis of the Environmental Condition of Reservoirs Using the Armenian Water Quality Index. "Water for

Sustainable Development in Central Asia", dedicated to the start of the International Decade of Action "Water for Sustainable Development, 2018-2028". Pp. 112-115.

Singh et al., 2011 – *Singh, R., Gautam, N., Mishra, A., Gupta, R.* (2011). Heavy metals and living systems: An overview. *Indian J Pharmacol.* 43(3): 246-253, doi: 10.4103/0253-7613.81505.

Song et al., 2013 – *Song, X.Q., Liu, L.F., Jiang, Y.J., Zhang, B.C., Gao, Y.P., Liu, X.L., Lin, Q.S., Ling, H.Q., Zhou, Y.H.* (2013). Disruption of secondary wall cellulose biosynthesis alters cadmium translocation and tolerance in rice plants. *Mol. Plant*. 6: 768-780.

Sukiasyan et al., 2020 – *Sukiasyan, A., Kirakosyan, A., Pirumyan, G.* (2020). Evaluation of heavy metal pollution in the vicinity of the Shnokh River by the geoaccumulation index. *Russ Journal of General Chemistry*. 90(13): 2659-2663. DOI: https://doi.org/10.1134/S1070363220130204

Sukiasyan et al., 2021– *Sukiasyan, A., Kroyan, S., Skugoreva, S., Kirakosyan, A., Ghazaryan, H.* (2021). Consequences of the impact of some industrial plants on the content of heavy metals in soils. *Theoretical and Applied Ecology*. 4: 90-97. DOI: 10.25750/1995-4301-2021-4-090-097.

Sukiasyan, 2018 – *Sukiasyan, A.* (2018). New approach to determining the environmental risk factor by the biogeochemical coefficients of heavy metals. *South of Russia: ecology, development*. 13(4): 108-118. DOI: 10.18470/1992-1098-2018-4-108-118.

Sukiasyan, Kirakosyan, 2020 – *Sukiasyan, A., Kirakosyan, A.* (2020). Ecological evaluation of heavy metal pollution of different soil-climatic regions of Armenia by biogeochemical coefficients. *DRC Sustainable Future: Journal of Environment, Agriculture, and Energy*. 1(2): 94-102. DOI: 10.37281/DRCSF/1.2.2

Sukiasyan, Pirumyan, 2018 – *Sukiasyan, A., Pirumyan, G.* (2018). Influence of the content of heavy metals in water and soil on the environmental stress of plants in different climatic zones of the Republic of Armenia. *Water and ecology: problems and solutions*. 2 (74): 87-94.

Tchounwou et al., 2012 – *Tchounwou, P.B., Yedjou, C.G., Patlolla, A.K., Sutton, D.J.* (2012). Heavy metal toxicity and the environment. *Exp Suppl.* 101: 133-64. doi: 10.1007/978-3-7643-8340-4_6

Tepanosyan et al., 2018 – *Tepanosyan, G., Sahakyan, L., Pipoyan, D., Saghatelyan, A.* (2018). Risk Assessment of Heavy Metals Pollution in Urban Environment. In (Ed.), Risk Assessment. IntechOpen. DOI: https://doi.org/10.5772/intechopen.70798

Third National Communication..., 2015 – Third National Communication on Climate Change according to the UN Framework Convention on Climate Change – Yerevan, 2015, 191 p. [Electronic resource]. URL: https://unfccc.int

Tutunjyan, Pirumyan, 2011 – *Tutunjyan, A.A., Pirumyan, G.P.* (2011). Ecological assessment of the pollution of some rivers in the southern basin of the Republic of Armenia. *Water: Chemistry and Ecology*. 3: 2-8. [Electronic resource]. URL: http://watchemec.ru/article/23541

Vodyansky, 2012 – *Vodyansky, Y.N.* (2012). Standard content of heavy metals and metaloids in soils. *Soil Science*. 3: 368-375.

Wuana, Okieimen, 2011 – *Wuana, R.A., Okieimen, F.E.* (2011). Heavy metals in contaminated soils: a review of sources, chemistry, risks and best available strategies for remediation. *ISRN*. 1-21: 402647. DOI: https://doi.org/10.5402/2011/402647

Yan et al., 2020 – *Yan, A., Wang, Y., Tan, S.N., Mohd Yusof, M.L., Ghosh, S., Chen, Z.* (2020). Phytoremediation: A Promising Approach for Revegetation of Heavy Metal-Polluted Land. Front. *Plant Sci.* 11: 359. DOI: 10.3389/fpls.2020.00359